WILEY

RESEARCH ARTICLE

The inferior occipital gyrus is a major cortical source of the face-evoked N170: Evidence from simultaneous scalp and intracerebral human recordings

Corentin Jacques[1,2] | Jacques Jonas[3,4] | Louis Maillard[3,4] | Sophie Colnat-Coulbois[3,5] | Laurent Koessler[3,4] | Bruno Rossion[1,3,4]

[1]Psychological Science Research Institute, Institute of Neuroscience, Université Catholique de Louvain, Louvain-la-Neuve, Belgium

[2]Department of Neuroscience, KU Leuven, Center for Developmental Psychiatry, Leuven, Belgium

[3]Université de Lorraine, CNRS, CRAN, F-54000 Nancy, France

[4]Université de Lorraine, CHRU-Nancy, Service de Neurologie, F-54000 Nancy, France

[5]Université de Lorraine, CHRU-Nancy, Service de Neurochirurgie, F-54000 Nancy, France

Correspondence

Bruno Rossion, CRAN, UMR 7039, CNRS - Université de Lorraine, Pavillon Krug (1er étage - entrée CC-1), Hôpital Central, CHRU Nancy - Centre Hospitalier Universitaire de Nancy, 29 Avenue du Maréchal de Lattre de Tassigny, 54000 Nancy, France
Email: bruno.rossion@univ-lorraine.fr

Funding information

Fédération Wallonie-Bruxelles, Grant/Award Number: ARC 13/18-053; Fonds de la Recherche scientifique, Grant/Award Number: PDR T.0207.16; Louvain Foundation

Abstract

The sudden onset of a face image leads to a prominent face-selective response in human scalp electroencephalographic (EEG) recordings, peaking 170 ms after stimulus onset at occipito–temporal (OT) scalp sites: the N170 (or M170 in magnetoencephalography). According to a widely held view, the main cortical source of the N170 lies in the fusiform gyrus (FG), whereas the posteriorly located inferior occipital gyrus (IOG) would rather generate earlier face-selective responses. Here, we report neural responses to upright and inverted faces recorded in a unique patient using multicontact intracerebral electrodes implanted in the right IOG and in the OT sulcus above the right lateral FG (LFG). Simultaneous EEG recordings on the scalp identified the N170 over the right OT scalp region. The latency and amplitude of this scalp N170 were correlated at the single-trial level with the N170 recorded in the lateral IOG, close to the scalp lateral occipital surface. In addition, a positive component maximal around the latency of the N170 (a P170) was prominent above the internal LFG, whereas this region typically generates an N170 (or "N200") over its external/ventral surface. This suggests that electrophysiological responses in the LFG manifest as an equivalent dipole oriented mostly along the vertical axis with likely minimal projection to the lateral OT scalp region. Altogether, these observations provide evidence that the IOG is a major cortical generator of the face-selective scalp N170, qualifying the potential contribution of the FG and questioning a strict serial spatiotemporal organization of the human cortical face network.

1 | INTRODUCTION

The human face is a highly complex, familiar, and socially critical stimulus in our visual environment. For these reasons, understanding the spatiotemporal organization of face processing in the human brain is a primary goal of cognitive neuroscience research. The neural basis of face processing has been intensively investigated for three decades with functional neuroimaging, first with positron emission tomography (Sergent, Ohta, & Macdonald, 1992) then with functional magnetic resonance imaging (fMRI; Puce, Allison, Gore, & McCarthy, 1995). The advent of fMRI, in particular, has allowed defining a set of regions in the occipito-temporal (OT) cortex of the typical human adult brain that respond significantly more to pictures of faces than nonface

objects. The most prominent and consistent of these face-selective regions have been identified in the lateral section of the middle fusiform gyrus (LFG, the functional area being termed the "fusiform face area" [FFA]; Kanwisher, McDermott, & Chun, 1997), the inferior occipital gyrus (IOG) on the lateral section of the occipital cortex ("occipital face area" [OFA], Gauthier et al., 2000), as well as the posterior superior temporal sulcus (pSTS; Puce, Allison, Bentin, Gore, & McCarthy, 1998). These regions are typically defined as forming the core of a distributed cortical face network in the human brain (Calder & Young, 2005; Duchaine & Yovel, 2015; Grill-Spector, Weiner, Kay, & Gomez, 2017; Haxby, Hoffman, & Gobbini, 2000 for reviews; see, e.g., Gao, Gentile, & Rossion, 2018; Rossion, Hanseeuw, & Dricot, 2012; Zhen et al., 2015 for extensive fMRI investigations of the human cortical face network). However, as fMRI provides a slow and indirect (i.e., hemodynamic) measure of neural

activity, the temporal organization of this network (i.e., when are these brain regions activated, for how long, etc.) remains largely elusive.

To provide complementary high temporal resolution information (at the expense of spatial precision), electrical potentials elicited by the sudden onset of face stimuli have also been recorded for decades from the human scalp with electroencephalography (EEG) (since Srebro, 1985). While early studies with few scalp electrodes emphasized a face-selective component recorded on the vertex (Cz electrode) at around 160–170 ms following the onset of a face stimulus (the vertex positive potential [VPP]; Botzel & Grusser, 1989; Jeffreys, 1989 for a review, see Jeffreys, 1996), the vast majority of EEG studies has focused on a prominent negative deflection peaking at the same latency over OT sites: the N170 (Bentin, McCarthy, Perez, Puce, & Allison, 1996; see also Botzel, Schulze, & Stodieck, 1995; George, Evans, Fiori, Davidoff, & Renault, 1996 for early studies; Rossion, 2014; Rossion & Jacques, 2011 for reviews). Studies using magnetoencephalography (MEG) have also recorded a similar "M170" component (e.g., Halgren, Raij, Marinkovic, Jousmaki, & Hari, 2000; Itier, Herdman, George, Cheyne, & Taylor, 2006; Liu, Higuchi, Marantz, & Kanwisher, 2000) which presents similar response properties as the N170, in particular a larger amplitude for faces than non-face object categories (Bentin et al., 1996; Ganis, Smith, & Schendan, 2012; Gao et al., 2013; Itier & Taylor, 2004; Rossion et al., 2000; Rossion & Jacques, 2008; Rousselet, Husk, Bennett, & Sekuler, 2008) and a substantial increase of both amplitude and latency to face stimuli presented upside down (Eimer, 2000; Itier et al., 2006; Itier & Taylor, 2004; Jacques & Rossion, 2007; Jacques, Schiltz, & Goffaux, 2014; Rossion et al., 1999; Rousselet, Mace, & Fabre-Thorpe, 2004; Sadeh & Yovel, 2010; see Rossion & Jacques, 2011 for review).

In order to characterize the spatiotemporal dynamics of face processing in the human brain, a number of authors have attempted to relate the face-evoked N170/M170 measured on the scalp to face-selective OT cortical regions defined in neuroimaging studies. Since the fusiform gyrus (FG) was the first region systematically associated with face-selective processing in neuroimaging studies (Kanwisher et al., 1997; Puce et al., 1995; Sergent et al., 1992), but also based on other sources of evidence (see below), the vast majority of studies consider that the N170/M170 primarily originates from the FG (see also the review of Yovel, 2016). Empirically, a first piece of evidence comes from early intracranial recording studies using electrocorticography (ECoG) in human epileptic patients, which reported a N170-like component (termed the N200) over the FG and inferior temporal gyrus, but not over the lateral IOG (Allison et al., 1994; see also Allison, Puce, Spencer, McCarthy, & Belger, 1999; McCarthy, Puce, Belger, & Allison, 1999; Puce, Allison, & McCarthy, 1999 for extensive reports). This work in fact provided the impetus for the subsequent recording of the face-selective N170 over the human scalp of typical individuals with the same paradigm and stimuli (Bentin et al., 1996). Second, a number of studies using various source localization approaches have emphasized the contribution of the posterior/middle FG (e.g., Botzel et al., 1995; Deffke et al., 2007; Gao et al., 2013; Halgren et al., 2000; Hoshiyama, Kakigi, Watanabe, & Miki, 2003; Mnatsakanian & Tarkka, 2004; Pizzagalli et al., 2002; Rossion, Joyce, Cottrell, & Tarr, 2003; Shibata et al., 2002; Swithenby et al., 1998;

Tanskanen, Nasanen, Montez, Paallysaho, & Hari, 2005; Watanabe, Kakigi, & Puce, 2003) or even of the anterior FG (Herrmann, Ehlis, Muehlberger, & Fallgatter, 2005) as neural sources of the N170/M170 and its increased amplitude to faces. Third, some studies have reported significant correlations between face-selective fMRI activity in the FG (i.e., FFA) and the amplitude of the N170 when manipulating noise levels applied to the face stimuli (Horovitz, Rossion, Skudlarski, & Gore, 2004). In the same vein, a simultaneous EEG–fMRI study found a significant correlation between the magnitude of face selectivity measured in ERPs at the peak of the 170 ms and in fMRI in the FG (Sadeh, Podlipsky, Zhdanov, & Yovel, 2010).

In the latter study (Sadeh et al., 2010), the authors also emphasized the lack of significant correlation between the electrophysiological face-selectivity index at 170 ms and fMRI face-selective activity in the IOG (i.e., OFA). In fact, this most posterior cortical face-selective region, usually located in the lateral section of the IOG, is rarely considered as a potential source of the face-evoked N170/M170 in source localization studies (e.g., Henson, Mouchlianitis, & Friston, 2009; Itier et al., 2006). Rather, based on the timing of effects of transcranial magnetic stimulation (TMS) on face processing tasks as well as correlations of fMRI and scalp EEG face-selective responses, it has been proposed that face-selective activity in the IOG peaks and is correlated with scalp EEG at an earlier latency, that is, at around 80–120 ms, during the time window of the P1 component preceding the N170 (Pitcher, Garrido, Walsh, & Duchaine, 2008; Pitcher, Walsh, Yovel, & Duchaine, 2007; Sadeh et al., 2010). According to this serial/hierarchical spatiotemporal view, face-selective responses would initially peak at around 100 ms (i.e., at the level of the P1/M1 component) in the IOG—possibly involved in extracting specific face parts (eyes, nose, mouth, etc.)—and feeding later into the FG where face-selectivity peaking at around 170 ms would reflect a holistic/configural representation of faces (Duchaine & Yovel, 2015; Pitcher, Walsh, & Duchaine, 2011; Yovel, 2016).

So far, this serial/hierarchical view of category-selective face processing has been challenged only by indirect evidence. First, time-resolved fMRI in the healthy brain indicates that the initial activation to slowly revealed faces emerges initially in the FG rather than in the IOG (Gentile, Ales, & Rossion, 2017; Jiang et al., 2011; Jiang, Badler, Righi, & Rossion, 2015). Second, EEG recordings in individuals with lesions of various face-selective OT cortical regions (OFA, FFA, or pSTS) suggest that multiple face-selective regions are likely involved in generating the scalp N170 (Dalrymple et al., 2011; Prieto, Caharel, Henson, & Rossion, 2011). Third, given the anatomical location of the FG with the majority of its cortical surface facing toward the inferior part of the head (Figure 1), the contribution of face-selective responses in this region to the scalp N170 recorded over the lateral OT scalp regions should be questioned. This geometrical incompatibility was in fact noted by Bentin et al. (1996) in their seminal study. Bentin et al. (1996) speculatively attributed the source of the N170 to the OT sulcus (OTS), pointing toward the lateral surface of the brain and scalp (see fig. 8 in Bentin et al., 1996). More recently, Rosburg et al. (2010) performed simultaneous intracranial and scalp recordings of ERPs to upright and inverted faces, using inversion as a functional marker of the N170. As amplitude and latency increase with inversion were revealed for the intracranial N170 recorded in the lateral IOG
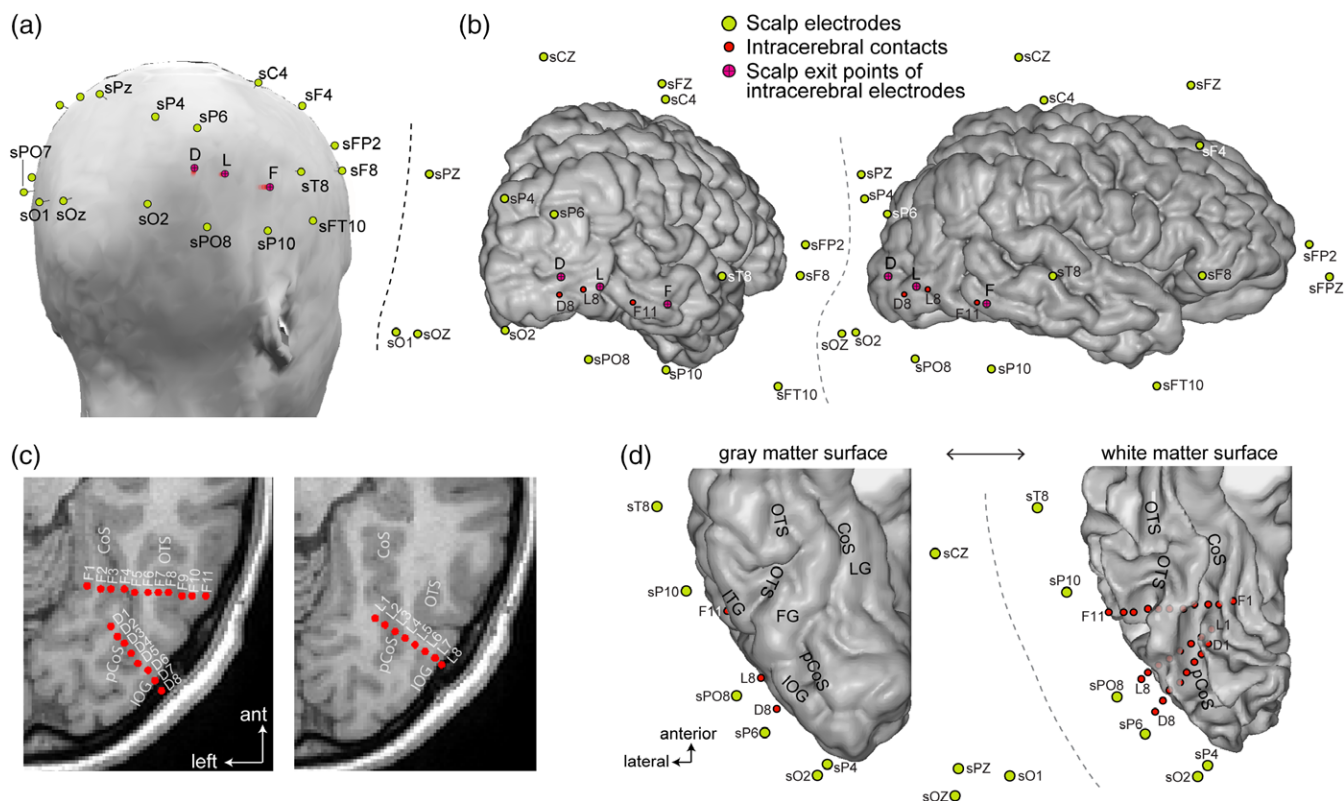
FIGURE 1 Simultaneous recording of scalp and intracerebral EEG. (a) Scalp view from the posterior right hemisphere showing the position of the scalp recording electrodes (shown in green) and the location on the scalp of the exit point of the three intracerebral electrodes (D, L, and F, shown as red dots). (b) Three/quarter posterior and profile views of three-dimensional (3D) reconstruction of the patient's right hemisphere cortical surface, showing the locations of the intracerebral electrodes (in red, only the most external contacts D8, L8, and F11 appear on the cortical surface) and the locations of the scalp electrodes (green). (c) Axial views of the posterior half of the right hemisphere of the patient, showing the locations of intracerebral contacts in the right OT cortex. Electrode L was slightly superior to D and F electrodes. (d) 3D ventral views of the posterior half of the right hemisphere of the patient, showing the anatomical location of the intracerebral contacts and scalp electrodes. The plots show the gray matter cortical surface (left) and the corresponding white matter surface (right). As intracerebral contacts penetrate the brain tissue, contacts are only visible when stripping away the gray matter and keeping only white matter surface (left). Abbreviations: FG = fusiform gyrus; IOG = inferior occipital gyrus; LG = lingual gyrus; OTS = occipito-temporal sulcus; (p)CoS = (posterior) collateral sulcus [Color figure can be viewed at wileyonlinelibrary.com]

but not in the FG, the authors concluded that the lateral IOG contributes primarily to the face inversion effect (FIE) observed in scalp recordings. Unfortunately, the use of few (n = 6) electrodes and a reference over the mastoid (i.e., close to OT regions) prevented from a direct investigation of the scalp N170 over OT regions in that study. Moreover, that study—similarly to the studies of Allison et al. (1994, 1999)—was performed with grids of electrodes applied on the cortical surface (ECoG) rather than with multicontact electrodes inserted directly in the brain volume (stereotactic EEG [SEEG], Talairach & Bancaud, 1973). Hence, Rosburg et al. (2010) observed only negative components intracranially, which were difficult to relate to the positivity that they observed simultaneously on the vertex, the VPP.

Here, we present a detailed report of a patient with rare SEEG recording of face-evoked responses inside both the IOG and LFG of the right hemisphere, together with simultaneous scalp EEG recording using multiple electrodes placed over the whole scalp, including the OT region. We examined the contribution of the IOG and LFG to the N170 measured on the scalp over OT regions. We asked the following questions: (a) can we find an intracerebral N170 response in the lateral IOG with similar response properties as the N170 measured on

the scalp OT region in the same patient? (b) are the SEEG responses in the IOG and the LFG correlated with the scalp OT N170? and (c) does the topology of electrophysiological responses and the cortical geometry of the FG region support a contribution of this region to the scalp OT N170? Addressing these issues should also shed light on the above-described serial/hierarchical spatiotemporal framework of the human cortical face network.

2 | METHODS

2.1 | Case description

KV is a right-handed female suffering from refractory occipital epilepsy related to a focal cortical dysplasia involving the right lingual gyrus (LG) and posterior collateral sulcus (pCoS). Her case was previously reported as evidence of a transient inability to recognize famous faces (Jonas et al., 2012), following intracerebral electrical stimulation of the face-selective region of the right IOG (OFA). That study was performed during a first SEEG implantation in 2010 to delineate the source and extent of the patient's epileptic seizures. During a second implantation

performed in 2011 with fewer intracerebral electrodes targeting the focal cortical dysplasia and surrounding cortical areas for therapeutic purposes, OFA stimulation caused a transient impairment at discriminating pictures of unfamiliar individual faces (Jonas et al., 2014). The present data set was also collected during this second implantation. The patient was 32 years old at the time of this second implantation.

The patient has never reported face recognition difficulties and has preserved memory and preserved visual perception (including faces and objects), as shown by stringent neuropsychological evaluations (Jonas et al., 2012). These electrophysiological investigations were part of the presurgical functional mapping of the patient. She gave written informed consent for these data to be used for research purpose according to the rules of the ethical committee of the Nancy University Hospital.

2.2 | Simultaneous intracerebral–scalp EEG recordings

The patient underwent simultaneous intracerebral (SEEG) and scalp EEG recordings. The colocations of these electrodes are shown in Figure 1. Besides the relatively dense spatial coverage of scalp electrodes for such a study (e.g., compared to six electrodes in Rosburg et al., 2010), the right OT cortex was well sampled with both intracerebral and surface electrodes.

2.2.1 | Intracerebral electrodes

The patient was stereotactically implanted with three multicontact intracerebral electrodes targeting the right ventral OT cortex, according to a well-defined and previously described procedure (Jonas et al., 2014; Salado et al., 2018). Each intracerebral electrode consisted of a cylinder of 0.8 mm diameter and contained 8–11 independent recording contacts of 2 mm in length separated by 1.5 mm from edge to edge and by 3.5 mm center to center. Electrode D (8 recording contacts, D1–D8) targeted the right ventral occipital cortex, from the lateral part of the IOG to the pCoS. Electrode F (11 contacts, F1–11) was located more anteriorly in the ventral OT junction, from the right inferior temporal gyrus to the LG, passing above the posterior FG. Electrode L (eight contacts, L1–L8) was located between electrodes D and F, also in the right occipital cortex but slightly above these electrodes. All intracerebral recording contacts were in direct contact with the gray matter, either located completely within the gray matter (e.g., contact L7 in the lateral IOG, Figure 1c,d) or in contact with both the white and the gray matter (e.g., contacts L5, F6, and F7). Note that, this kind of electrode implantation is rare in clinical practice, where most epileptic patients are implanted with more anterior electrodes to sample the temporal lobe.

2.2.2 | Scalp electrodes

Simultaneous scalp EEG recordings were acquired with 28 Ag/AgCl electrodes of 10 mm diameter placed according to the 10–20 system (Figure 1, see Koessler et al., 2015; Seeck et al., 2017) using sterile procedures, with a particular spatial coverage of bilateral OT regions. Here, they are referred to with the prefix "s" for scalp (e.g., sPO8 for PO8). Some of the posterior electrodes were slightly displaced relative to the 10–20 positions to keep them away from the penetrating point of the intracerebral electrodes (Figure 1). Scalp electrode positions

were determined using a three-dimensional digitizer system (3SPACE and FASTRAK; Polhemus, Colchester, VT). Note that the signal from electrode sP8 was not usable because of excessive noise and the impossibility to safely replace it during the long-term monitoring. However, electrodes sPO8, sP10, sO2, and sPO6 allowed a good coverage over the right OT cortex.

2.2.3 | Recordings

Simultaneous SEEG–scalp EEG signals were recorded at a 1,024 Hz sampling rate with a 128 channel amplifier (SD LTM 128 Headbox; Micromed, Mogliano Veneto, Italy). The reference electrode was a prefrontal midline surface electrode (FPz). The recording of the experiment reported here was performed 2 days after the scalp electrode placement.

2.3 | Stimuli and procedure

The methods used here (stimuli, procedure) were the same as in a previous scalp EEG study (Prieto et al., 2011). Stimuli were 30 photographs of front view, upright, unfamiliar faces with neutral expression (15 females). They were cropped to remove external features (hair and ears) and shown without glasses, facial hair, or makeup. Faces were equalized for global luminance. They were displayed at approximately $3° \times 4°$ of visual angle. An additional set of 30 stimuli was created by vertically flipping the 30 face images (inverted faces). We chose to compare the response to upright faces to the exact same stimuli upside down because inverted faces offer the best control for low-level visual properties (as compared to other nonface object categories). Moreover, inversion leads to clear and undisputed increases of amplitude and latency of the N170 (e.g., Eimer, 2000; Rossion et al., 1999; see Rossion & Jacques, 2011 for review).

Upright and inverted faces were presented in a random order using E-prime 2. In each trial, a fixation point displayed at the center of the screen for 100 ms, followed approximately 300 ms (randomized between 200 and 400 ms) later by the presentation of a face (upright or inverted) stimulus during 300 ms. The offset of this stimulus was followed by an intertrial interval of about 1,700 ms (1,600–1,800 ms). Patient KV had to press one response key on a computer keyboard if the stimulus was upright and another key on the stimulus was inverted. She was asked to maintain eye gaze fixation to the center of the screen and to respond as accurately and as fast as possible. KV performed 90 trials per condition in one session (30 stimuli in each set repeated three times each; 180 trials in total).

2.4 | Data processing and analyses

2.4.1 | EEG preprocessing

All analyses were performed using Letswave 5 (Mouraux & Iannetti, 2008) and MATLAB v7.8 (The MathWorks Inc., Natick, MA). Continuous EEG data were epoched in segments centered on stimulus onset (−1 to 1 s). Epochs were then DC corrected and low-pass filtered at 25 Hz (zero-phase shift Butterworth filter, order 4). Noisy epochs, epochs containing blink artifacts or large epileptic spikes—in which signal amplitude at any point in the time window from −0.2 to 0.6 s was above or below 5.5 times the SD computed across all trials for

each time sample—were discarded. If the rejection threshold was exceeded at one channel, then the epoch was rejected for all (i.e., scalp and intracranial) channels. This led to the rejection of 18% of the epochs. Additional expert visual inspection for potential remaining small epileptic spikes in the window of interest did not lead to further epoch rejection. Epochs were then baseline corrected by subtracting the amplitude in the 0.1 s prestimulus time window, and then averaged.

2.4.2 | N170/P170 analyses

N170/P170 peak was measured on intracerebral contacts and scalp electrodes with an identifiable ERP component within a time window of 140–200 ms (165–225 ms for SEEG contact F8, see below). The amplitude of the peak at each channel was quantified as the mean signal amplitude within a ±10 ms time window centered on the peak latency. The peak was identified automatically as the local minimum/maximum within a time window of 140–200 ms (165–225 ms for SEEG contact F8). Statistical comparisons between the N170 measured in the upright face versus inverted face condition were performed at each channel. We used a permutation test for the N170 amplitude (e.g., Jacques et al., 2014; Rousselet et al., 2008), by comparing the actual amplitude difference to a distribution of differences under the null hypothesis obtained by randomly shuffling the condition label for each trial (before computing the difference) 10,000 times. To statistically assess the latency inversion effect, we used a jackknife procedure (Miller, Patterson, & Ulrich, 1998) in which the *SD* of the single-trial latency is estimated (and corrected by multiplying the jackknife *SD* by the number of epochs minus one) separately for each condition, by systematically leaving-out one trial at a time before computing the ERP average and measuring the peak latency. The mean latency and *SD* for each condition was used to compute a *t* test. For the latency comparison, we upsampled single-trial data by a factor of 10 (i.e., to 10,240 Hz using cubic interpolation) to avoid always obtaining the same peak latency for all jackknife samples. For intracerebral contacts where the effect of inversion (amplitude and latency) was tested (*N* = 23), we used a Bonferroni correction to account for multiple comparisons.

2.4.3 | Correlation between intracerebral and scalp EEG signals in the N170 time window

We examined the relationship between the N170 peak latency and amplitude in intracerebral relative to scalp EEG recordings using a correlation approach, in the following way: (a) a subsample of 15 trials (out of 74 in the upright face condition) was randomly selected (without replacement); (b) these trials were averaged for each channel (an average over a subset of trials was used because the N170 could not be identified in single trials on scalp electrodes); (c) in the resulting averaged EEG segment, for each channel, the peak was identified as the local minimum or maximum amplitude in a 140–200 ms (165–225 ms for SEEG contact F8) time window (when no local maximum/minimum was present the derivative was computed, and the point closest to zero was considered as the peak) and the peak amplitude and latency values were stored; (d) steps a to c were repeated 5,000 times to obtain a distribution of amplitudes and latencies

measured at all channels in corresponding subsets of 15 trials, and (e) the resulting 5,000 amplitude and latency data points for each channel were used to quantify the relationship (using Pearson's coefficients) across all pairs of channels, respectively, for the amplitude and the latency of the N/P170. Correlation coefficients were tested against chance level using a permutation test, repeating steps a to e (see above) 4,000 times, shuffling the order of trials at each permutation so that correlations across channels were measured between unmatched subsets of trials. At each of the 4,000 permutation cycles, we stored the maximum Pearson's coefficient across all intracerebral–scalp EEG pairs of channels to generate a permutation distribution (i.e., distribution of coefficients obtained by chance) which corrects for multiple comparisons (Nichols & Holmes, 2001). For each pair of channel, the actual Pearson's coefficient was then compared to the permutation distribution to derive a *p* value. Only significant correlations (*p* < .05, i.e., corrected for multiple comparisons) observed in at least two neighboring scalp electrodes (i.e., within a radius of 5 cm from each other) were considered.

3 | RESULTS

3.1 | Patient KV shows typical FIE on the scalp-N170 component

The visual presentation of upright face images elicited robust biphasic ERP responses over the patient's scalp during the first 200 ms following stimulus onset (Figure 2a). The shape, latency, and scalp distribution of these early ERP responses were similar to that observed in typical adult participants during foveal stimulation (Bentin et al., 1996; Eimer, 2000; Ganis et al., 2012; Itier & Taylor, 2004; Jacques et al., 2014; Rossion & Jacques, 2011; Rousselet et al., 2004, 2008). A first positive deflection peaking over broad bilateral OT regions at about 110–120 ms (P100) was followed by a negative deflection (N170) maximal over bilateral OT regions (Figure 2b) at about 160–170 ms (162 and 167 ms on sPO8 and sO2, respectively, for the right hemisphere; 169 and 176 ms on sPO7 and sO1, respectively, for the left hemisphere).

Notably, the N170 was strongly increased both in amplitude and latency in response to images of inverted faces (Figure 2), which is the typical signature of the FIE on the scalp-recorded N170 component as revealed by numerous EEG studies in healthy adults (Itier et al., 2006; Itier & Taylor, 2004; Jacques et al., 2014; Jacques & Rossion, 2007; Rossion et al., 1999, 2000; Rousselet et al., 2004). Over right OT channel sPO8, the peak amplitude of the N170 was 3.4 μV larger in response to inverted (−6.3 ± 9 μV) compared to upright faces (−2.9 ± 7.6 μV). The amplitude increase following face inversion was largest at right OT channels (Figure 2b). Testing 12 individual posterior scalp electrodes revealed a significant amplitude increase with inversion at four OT channels in the right hemisphere (sO2, sPO8, sP10, and sP6, *ps'* = 0.0077–0.032, one-tailed permutation test, uncorrected) and one OT channel in the left hemisphere (PO7, *p* = .042). When averaging across four OT channels, the amplitude increase was significant in the right hemisphere (3.01 μV, *p* = .014) but not in the left hemisphere (1.2 μV, *p* = .18). Similarly, the N170 peak latency at right OT channel
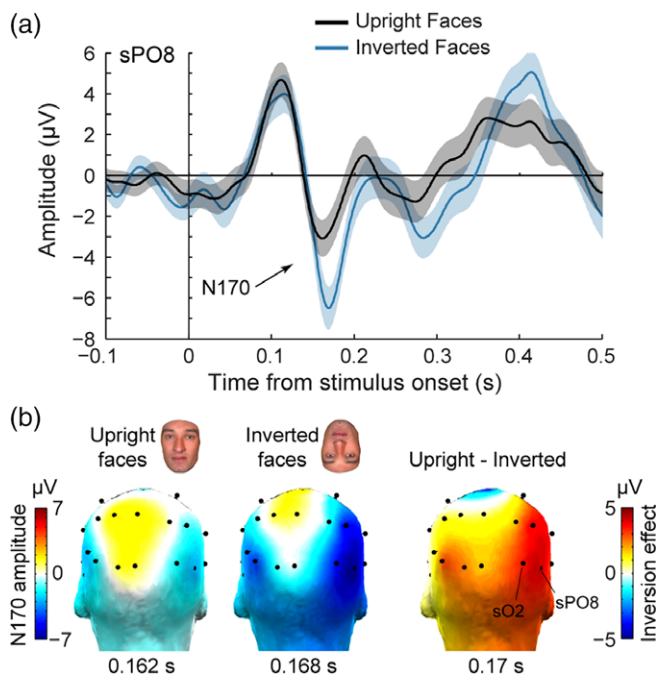
FIGURE 2 Scalp response to upright and inverted faces in patient KV. (a) Averaged ERP responses to upright and inverted faces at a single right hemispheric occipito-temporal (OT) scalp electrode (sPO8) in patient KV (see scalp location in panel B). Shaded regions are *SE* across trials. The large N170 component, peaking at around 170 ms, is increased in amplitude and latency for inverted faces compared to upright faces. (b) Patient KV's scalp topographical distribution of the N170 peak for upright faces (left), inverted faces (middle), and the difference between upright and inverted face conditions (right). Topographical maps are displayed from the back of the head at the latency of the peak component or peak difference (latency indicated below each map). These scalp topographies show typical N170 and N170 inversion effect of posterior OT regions, with a right hemispheric dominance [Color figure can be viewed at wileyonlinelibrary.com]

sPO8 was 7 ms later to inverted (170 ms) compared to upright (163 ms) faces. The latency increase following face inversion was significant at five right OT channels (sO2, sPO8, sP10, sP6, sT8, *p*s' = 0.019–0.0006 uncorrected, latency IE range: 6–11 ms) and one left OT channel (sPO7, *p* = .007, latency IE: 5 ms). Together, these observations indicate that patient KV's electrophysiological response to faces over OT scalp regions are typical compared to normal healthy adults.

3.2 | Corresponding N170 properties between right OT scalp region and lateral inferior occipital cortex

ERP responses to face images were also observed in intracerebral recordings, in most recording contacts in the ventral and lateral sections of the OT and posterior temporal cortex (Figure 3). We specifically focused on the contacts exhibiting a prototypical biphasic response during the first 200 ms following stimulus onset and resembling responses measured on the scalp. These biphasic responses consisted in either a P100–N170 sequence of ERP components or its polarity reversal N100–P170, and were observed in all contacts of electrodes D and L (occipital cortex: LG, pCoS, and IOG) and in 5 out of 11 contacts of electrode F (contacts F1, F2, and F5 in

the lingual gyrus and the CoS, contacts F6 and F7 above the FG). All contacts with a N170 or P170 showed a robust FIE manifested as an increase in the amplitude and/or the latency of the N170/P170 component in response to inverted compared to upright faces (Figure 4). Across these contacts, the mean amplitude increase (±std across contacts) due to face inversion was 31 ± 14.2 μV, with a range of 11.5–58.8 μV (Figure 4a). The amplitude increase was significant (*p* < .05 Bonferroni corrected) at all contacts except F6 and F7. Across contacts, the mean latency increase for inverted faces was 6 ± 2.1 ms, with a range of 1.7–10.9 ms (Figure 4b). The latency increase was significant (*p* < .05 Bonferroni corrected) at all contacts except D1 and F1 (although the latency increase was significant on D1 if uncorrected: latency increase = 6.1 ms, *p* = .008 uncorrected). In addition to these SEEG contacts, we also considered contacts F8 and F9 located in the OTS (Figure 1c,d). These contacts did not display an early biphasic electrophysiological response, but showed a negative component around the time window of the N170 (Figure 3a), although with a slightly delayed peak latency as compared to lateral contacts of the L and D electrodes (198 ms in F8 and 182 ms in F9 in response to upright faces, Figure 4b). Amplitudes at these contacts were not significantly different for upright relative to inverted faces (*p* = .3 uncorrected, Figure 4a), but there was a significant latency increase with inversion in F8 (*p* < .0001, Bonferroni corrected), not F9 (*p* = .9 uncorrected, Figure 4b).

Importantly, specifically over the most external contacts of the D and L electrodes (D7-8 and L7-8) in the external surface of the lateral section of the IOG, responses to upright and to inverted faces were remarkably similar to responses measured over nearby scalp right OT channels (sPO8, sO2, sP10, and sP6). Indeed, the morphology, polarity, and latency of the negative component measured in lateral IOG match the polarity and latency of the N170 measured on scalp right OT channels both for upright and inverted faces (Figures 3 and 4). First, only D7-8 and L7-8 showed a polarity of the ERP components matching the polarity measured on the scalp (i.e., P1–N170, Figure 3a,b). The negative polarity "N170" was specifically recorded on these contacts. Moving toward more medial/deep intracerebral contacts in the posterior CoS (L1–L6 and D1–D6), there was a sudden shift in the polarity of both the P100 and N170 so that the P100 becomes an N100 and the N170 becomes a P170 (Figure 3a,b). This shift occurred between contacts D7 and D6, and L7 and L6, that is within the lateral part of the right IOG, with D7/L7 located close to the superficial layer of the cortex and D6/L6 in contact with the deeper part of the lateral IOG close to the posterior CoS. The polarity shift is best illustrated when visualizing the ERP waveforms as in the upper row of Figure 3a (e.g., contacts L8 and L6) or when visualizing the amplitude of the N170/P170 as colored dots as in Figure 3b (color changes from blue to red between contacts D7/L7 and D6/L6). A P170 of similar latency was also measured in contacts of electrode F located in the OTS, above the LFG (F6, F7, Figures 3b,c and 4b). Second, the latency of the scalp N170 to upright faces in right OT regions was very similar to that measured in lateral IOG (Figures 3c and 4b). Collapsing across face orientation, the mean N170 latency was 166 ± 4 ms for right OT scalp regions and 162 ± 5 ms for lateral IOG contacts (average of D7-8 and L7-8). In contrast, the P170
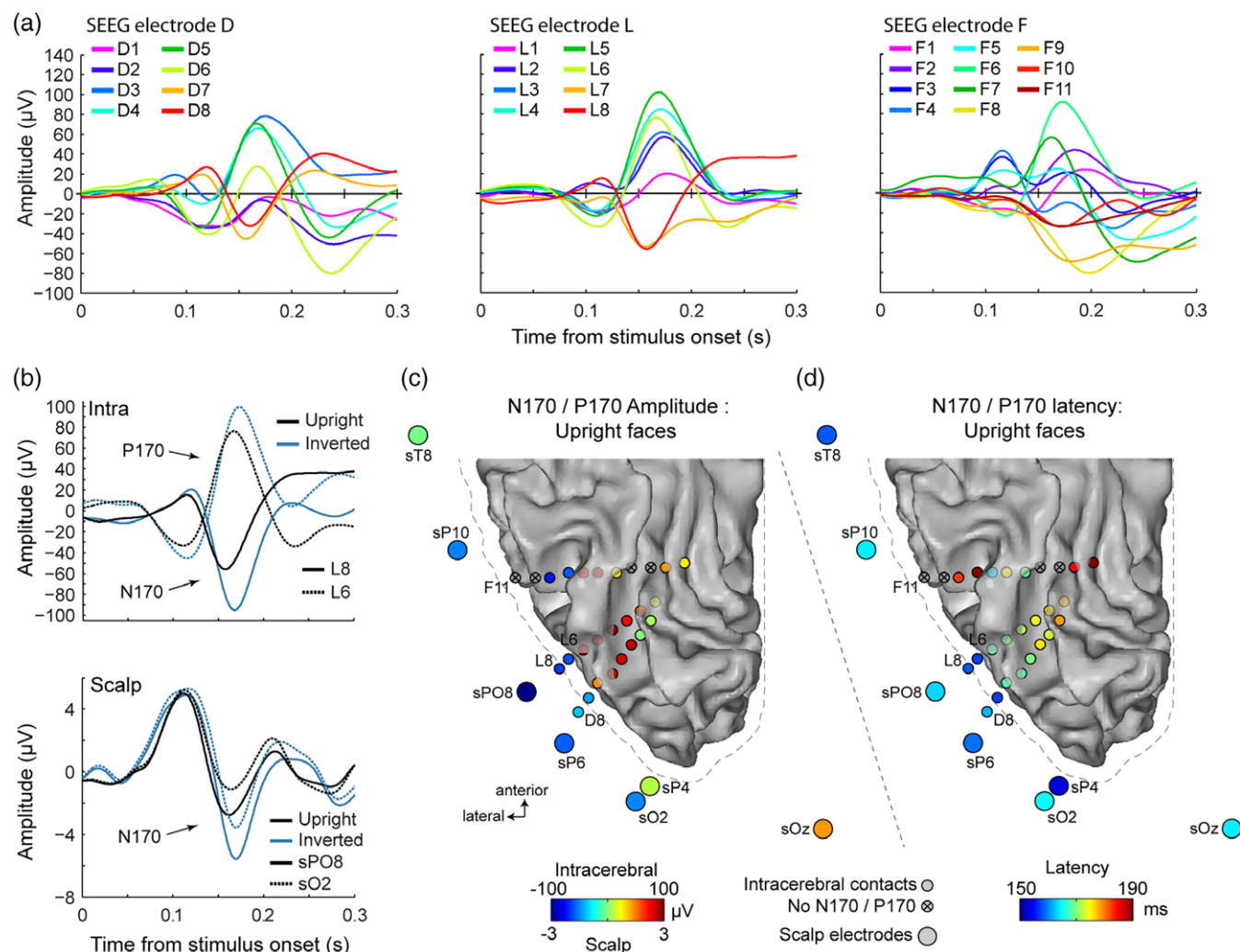
FIGURE 3 Intracerebral and scalp N170/P170 response to faces. (a) Averaged ERP responses to upright faces recorded at all 27 intracerebral recording contacts. Waveforms are displayed superimposed separately for the three multicontact electrodes (D, L, and F). (b) Top: averaged ERP responses to upright and inverted faces at two intracerebral contacts of electrodes L in the superficial part of the lateral inferior occipital gyrus (IOG) (L8) and in the deeper part of the lateral IOG close to the posterior collateral sulcus (L6). See panel B for their location. ERPs at these two contacts manifest an opposite polarity such that an N170 is measured in L8 and a P170 is measured in L6. Bottom: ERPs at two right occipito-temporal scalp electrodes near the intracerebral contacts shown above. Note the scale difference between intracerebral and scalp responses but the similarity in N170 latency. (c) Ventral view of the posterior half of the patient KV's right hemisphere (white matter surface with the gray matter surface shown as a dotted gray outline) together with intracerebral contacts (small circles) and selected surrounding scalp electrodes (large circles). The closest scalp electrodes to intracerebral contacts D8 and L8 were sPO8, sO2, sP10, and sP6 (Euclidian distance to D8 = 27, 26, 51, and 32 mm, respectively; Euclidian distance to L8 = 28, 35, 45, and 33, respectively). Channels are colored as a function of the amplitude of the N170/P170 for upright faces, measured as the mean amplitude in a ±10 ms around the peak. Note the difference in the color scale used for scalp and intracerebral data. (d) Same convention as for panel B but representing the N170/P170 latency for upright faces [Color figure can be viewed at wileyonlinelibrary.com]

recorded more medially (L1–L6 and D1–D6) peaked later overall (174 ± 5 ms) and progressively increased from more lateral to more medial contacts (Figure 4b). This latency difference between the N170 measured in the lateral IOG (D/L7-8) and adjacent more medial contacts (e.g., D/L5-6) suggests that the neural sources of the N170 measured in lateral IOG and P170 measured more medially might be, at least partly, different.

In summary, the similarity in polarity, latency, and inversion effect between the N170 measured on the scalp right OT regions and the N170 recorded on intracerebral lateral D and L contacts suggests that these scalp N170s arise from underlying neural sources in lateral IOG.

3.3 | Direct correlations of N170 latency and amplitude between scalp and intracerebral recordings

To more formally and directly determine the contribution of intracerebral sources to the N170 measured on the scalp, we quantified the correspondence of the N170 latency and amplitude between scalp and intracerebral recordings using a correlation approach.

First, we correlated the EEG peak *amplitude* during the N/P170 time window (i.e., 140–200 ms) across intracerebral contacts and scalp electrodes (Figure 5a). These analyses confirmed our hypothesis that N170 measured at OT scalp electrodes mainly arises from regions in lateral IOG. The highest and most consistent scalp-intracerebral correlations of EEG amplitude in the N170 window occurred between
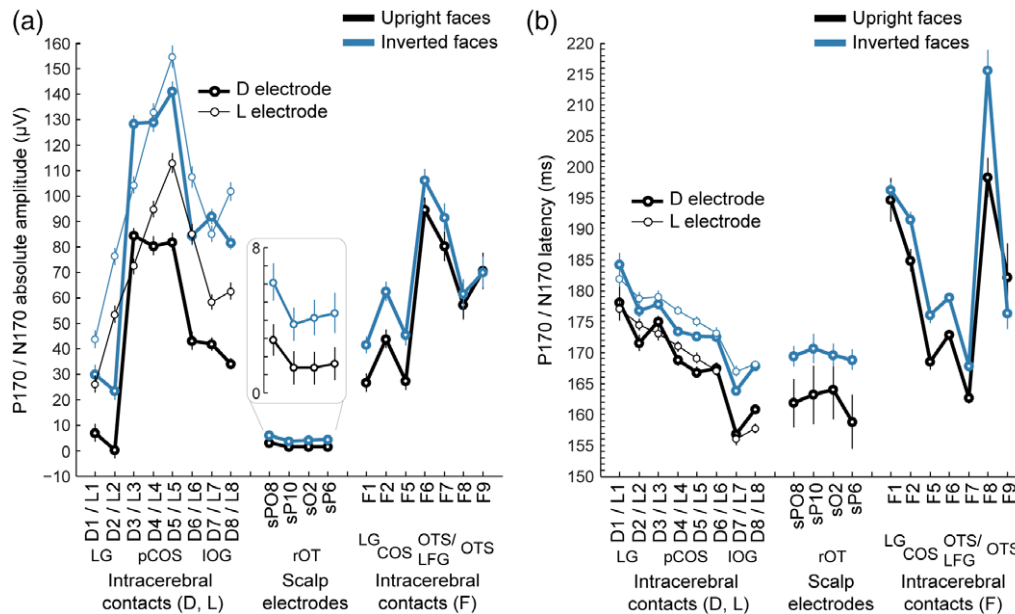
FIGURE 4 Intracerebral and scalp N170 amplitude and latency to upright and inverted faces. (a) The plot shows the absolute value of the peak amplitude of the N170/P170 measured at intracerebral contacts and right occipito-temporal scalp electrodes in response to upright and inverted faces. Error bars are *SE* of the mean. Amplitude at scalp OT channels is also displayed on a secondary scale in the square inset. (b) Same as for panel a but showing N170/P170 peak latency [Color figure can be viewed at wileyonlinelibrary.com]

intracerebral contacts in the lateral IOG (contacts D7-8, L7-8) and scalp electrodes distributed over bilateral OT and posterior parietal regions. Statistics indicate that the N170 amplitude measured at these four intracerebral contacts was significantly ($p < .05$, corrected for multiple comparison) correlated with a broad group of 11 scalp electrodes (mean Pearson's coefficient across 11 electrodes = 0.53 ± 0.05, range: 0.43–0.64, Figure 5b) for contacts D7-D8, and a group of five scalp electrodes (mean Pearson's coefficient across electrodes = 0.45 ± 0.03, range: 0.42–0.50, Figure 5b) for contacts L7-L8. When including the five common right OT scalp electrodes (sO2, sP4, sOZ, sP6, and sPO8) across D7-8 and L7-8, correlations were significantly ($t(4) = 15.401$, $p < .001$) higher with intracerebral contacts D7-8 ($r = 0.58 ± 0.03$) than with contacts L7-8 ($r = 0.45 ± 0.03$). Across the four intracerebral contacts (i.e., D7-8 and L7-8), correlations were also strongest with right posterior OT scalp regions (sP6, sPO8, sO2, sOZ, and sP4; mean Pearson's r coefficient = 0.52 ± 0.08, Figure 5) and were significantly stronger in scalp channels in the right OT (sP6, sPO8, s02, sP10, and sP4; mean $r = 0.5 ± 0.09$) compared to left OT (sP5, sPO7, s01, sP9, and sP3; mean $r = 0.38 ± 0.12$; $t(8) = 2.27$, $p = .027$, one-tailed). Significant correlations of left OT sites with right OT SEEG contacts mostly likely reflect an indirect correlation between the right and left hemispheres, in line with findings of interhemispheric connectivity of OT regions during face processing (Yang, Qiu, & Schouten, 2015). In the present study, these interhemispheric correlations are likely related to the commonality of input, early visual processing stages, and current state of the system when the image appears on the screen. In addition, correlations of 14 bilateral posterior scalp electrodes with intracerebral contacts D7-8 or L7-8 were significantly stronger than with directly adjacent contacts D6 (mean $r = 0.22$; D6 vs. D7-8: $t(13) = 10.2$, $p < .0001$) and L6 (mean $r = 0.13$; L6 vs. L7-8: $t(13) = 8.5$, $p < .0001$). Moreover, and in line with these latter observations, the correlations

of N/P170 amplitude between lateral contacts D7-8 and L7-8, as well as between medial contacts D5-6 and L5-6 were much higher (mean r for D7-8/L7-8 = 0.92, mean r for D5-6/L5-6 = 0.93) than correlations between lateral and medial contacts (D6-D7: $r = 0.19$; L6-L7: $r = 0.13$). This suggests that the neural sources generating the N170 and P170 in lateral IOG and adjacent posterior CoS (D5 and L5) are mostly independent.

Second, we correlated the EEG peak *latency* during the N/P170 time window across intracerebral and scalp electrodes (Figure 6a). This analysis confirmed that the lateral IOG is a prominent neural source of the N170 measured at right OT scalp electrodes. We observed a specific pattern of positive correlations between contacts D7-8, L7-8, and OT scalp electrodes with a strong right hemispheric dominance. Statistics indicated that N170 peak latency at these four intracerebral contacts were significantly correlated with a cluster of 3 to 6 scalp right OT electrodes (Figure 6b, mean Pearson's coefficient across electrodes = 0.39 ± 0.04, range: 0.30–0.49). Across 6 right OT scalp electrodes (sP6, sPO8, s02, sOz, sP10, and sP4), Pearson's coefficients were slightly larger for contacts D7-8 (mean r across contacts = 0.39; range: 0.3–0.49) than for contacts L7-8 (mean r = 0.33; range: 0.25–0.41). In contrast, correlations of the same scalp electrodes with directly adjacent intracerebral contacts D5-6 and L5-6 in the deep part of the IOG and the posterior CoS were around zero (mean $r = 0.02 ± 0.04$; range: −0.11 to 0.04).

For these contacts in the lateral IOG (i.e., D7-8 and L7-8), correlation coefficients between N170 peak latency were strongest at scalp electrodes in right OT, closest to the location of the corresponding intracerebral contacts (sPO8, sP6, sO2, sP4, sOz, and sP10). Moreover, for all four intracerebral contacts, correlations with posterior scalp electrodes were significantly stronger in the right hemisphere (mean r across 4 contacts/6 electrodes = 0.35) compared to the left hemisphere (mean r = 0.10; $ps < 0.001$).
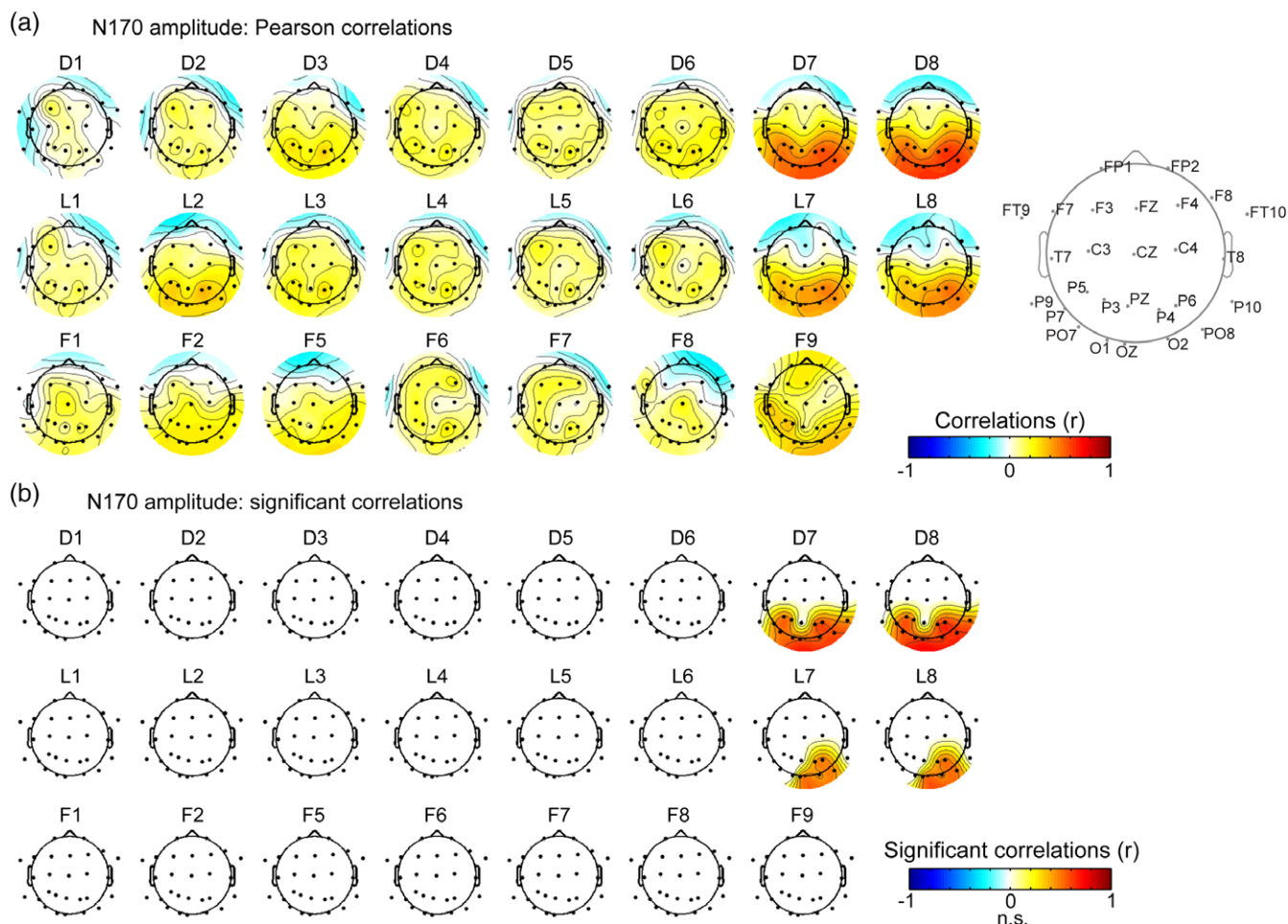
FIGURE 5 Correlations between intracerebral and scalp N170 amplitude to upright faces. (a) Scalp topographical maps (view from above the head) of the unthresholded Pearson correlation coefficients between the peak amplitude in the N170 time window measured at each intracerebral contact and each scalp electrode. Each map represents the correlations of one intracerebral contact with all scalp electrodes. Different intracerebral electrodes (D, L, and F) are shown in rows, and adjacent recording contacts are shown in columns (see Figure 1 for anatomical location of the contacts). Scalp electrodes' labels are shown on the right schematic head plot ("s" in front of the label is omitted for readability). (b) Topographical maps showing only significant correlation coefficients ($p < .05$, corrected for multiple comparisons). White indicates no significant correlation [Color figure can be viewed at wileyonlinelibrary.com]

These N170 latency analyses also revealed that while latency correlations between lateral contacts D7-8 and L7-8, as well as between medial contacts D5-6 and L5-6 were high (mean r for D7-8/L7-8 = 0.88, mean r for D5-6/L5-6 = 0.92), the N170 latencies were weakly correlated between lateral and medial contacts (D6-D7: $r = 0.3$; L6-L7: $r = 0.16$). Together with the similar observation made for the N/P170 amplitude, these observations support the view that although the N170 measured at the most lateral contacts in IOG (D7-8 and L7-8) and the P170 measured in adjacent contacts have very similar latencies (161 and 170 ms for N170 and P170, respectively, Figure 4), these components reflect the activity of separate neural sources. These analyses suggest again that only the most lateral source(s) (D7-8 and L7-8) contribute to the N170 measured on the scalp.

3.4 | Potential contribution of the LFG to OT scalp N170

The present data set shows that the right lateral IOG largely contributes to the N170 recorded on the scalp. We next examined whether the current data support an additional contribution of the LFG to the

scalp OT N170. In KV, two contacts of intracerebral electrode F (F6 and F7) were located just 8 mm above the inferior surface of the LFG (Figure 7). Importantly, these two contacts exhibited a positive component peaking during the N170 time window ("P170"), and which latency was significantly increased by face inversion.

Our data suggest that in the current patient, the LFG does not contribute or contributes minimally to the OT scalp N170. First, we observed no specific correlation between the P170 (latency or amplitude) measured at F6 or F7 and the N170 measured on the scalp OT regions. Second, we rule out that the electrical field generating this P170 is parallel to the main axis of the F electrode (i.e., with a medio-lateral orientation pointing to the lateral OT scalp region) for two reasons: (a) a P170 or N170 of similar morphology as in F6-F7 was not measured at adjacent sites in the OTS (F8-9: negative component of longer duration and later latency) and CoS (F4-5: different morphologies), and (b) there was no significant correlation between N170 latency measured in contacts F6-F7 and adjacent contacts F5 and F8 (mean r across pairs of electrodes = -0.1 ± 0.14). This indicates that responses measured in contacts F6-F7 do not arise from an equivalent dipole oriented roughly parallel to the F electrode. Rather, we
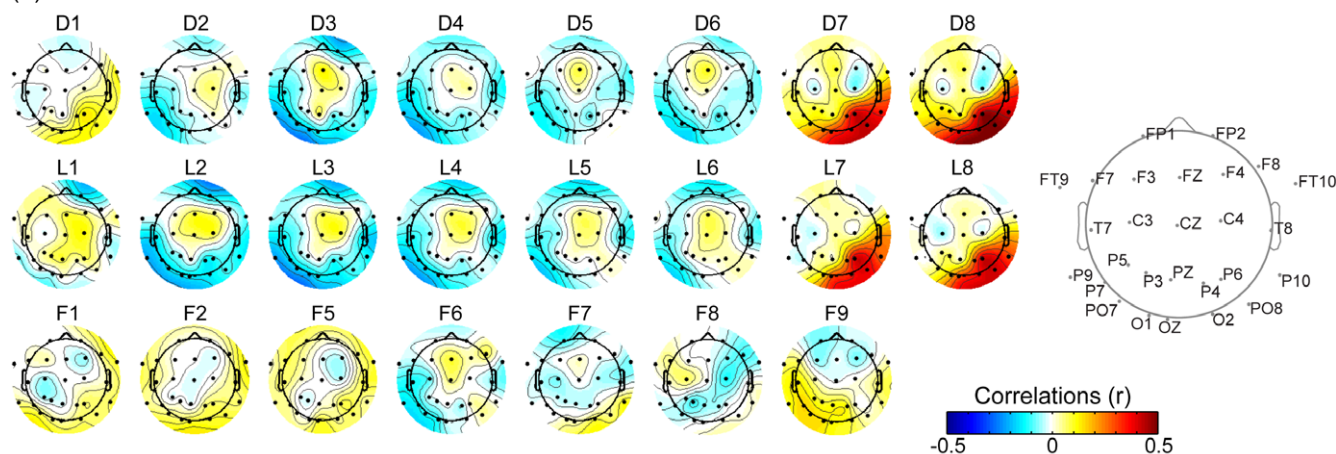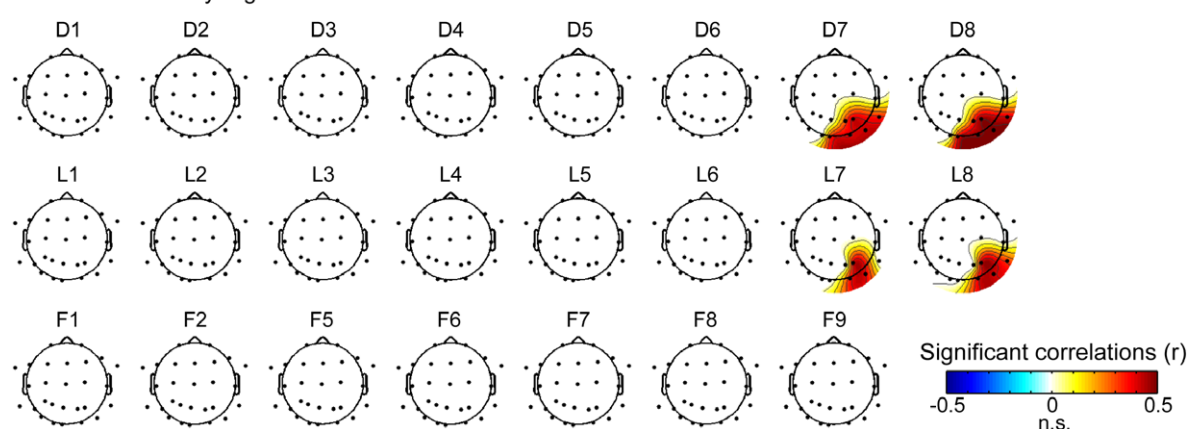
FIGURE 6 Correlations between intracerebral and scalp N170 latency to upright faces. (a) Scalp topographical maps (view from above the head) of the unthresholded Pearson correlation coefficients between the peak latency in the N170 time window measured at each intracerebral contact and each scalp electrode. Each map represents the correlations of one intracerebral contact with all scalp electrodes. Different intracerebral electrodes (D, L, and F) are shown in rows, and adjacent recording contacts are shown in columns (see Figure 1 for anatomical location of the contacts). Scalp electrodes' labels are shown on the right schematic head plot ("s" in front of the label is omitted for readability). (b) Topographical maps showing only significant correlation coefficients ($p < .05$, corrected for multiple comparisons). White indicates no significant correlation [Color figure can be viewed at wileyonlinelibrary.com]

hypothesize that the P170 measured in these contacts is generated from an equivalent dipole in the LFG located just below and oriented along a roughly vertical axis, pointing toward the bottom of the head and not toward the scalp lateral surface.

4 | DISCUSSION

4.1 | Summary and generalizability of our observations

The unique data set reported here points to the lateral section of the right IOG as a major cortical source of the scalp N170, a component evoked by the sudden onset of face stimuli and which has been described in hundreds of studies to characterize the functional properties of human face perception (Rossion & Jacques, 2011 for review) as well as its impairment in various neurological and psychiatric diseases (Feuerriegel, Churches, Hofmann, & Keage, 2015 for review). This conclusion is based on three key observations. First, the large N170 component elicited on recording contacts lying at the cortical surface

of the lateral IOG (D8 and L8) or inside the IOG gray matter (D7 and L7) (Figure 1), 3–4 cm away from scalp electrodes over the OT regions where the largest N170 is recorded in the patient and in typical healthy individuals. Second, the functional properties of this intracerebral component, that is, its characteristic negative polarity and peak latency at 170 ms, as well as its large and specific increase in both amplitude and latency for inverted faces, a consistent marker of N170 face specificity reported in tens of scalp recording studies as cited above, as well as in a previous intracranial study (Rosburg et al., 2010). This observation directly contradicts the view that upright and inverted faces are represented in a similar manner in face-selective regions in the IOG (Pitcher et al., 2011; Yovel, 2016). Third, thanks to the original simultaneous scalp recording with a (good) coverage over OT regions, the observation of a striking similarity between the intracerebral and scalp N170s in terms of mean latency and sensitivity to face inversion, as well as across-trial correlations of amplitude and latency.

These observations were possible thanks to a rare case of simultaneous intracerebral–scalp EEG recording where we had both a simultaneous coverage of the lateral IOG and the LFG and a relatively
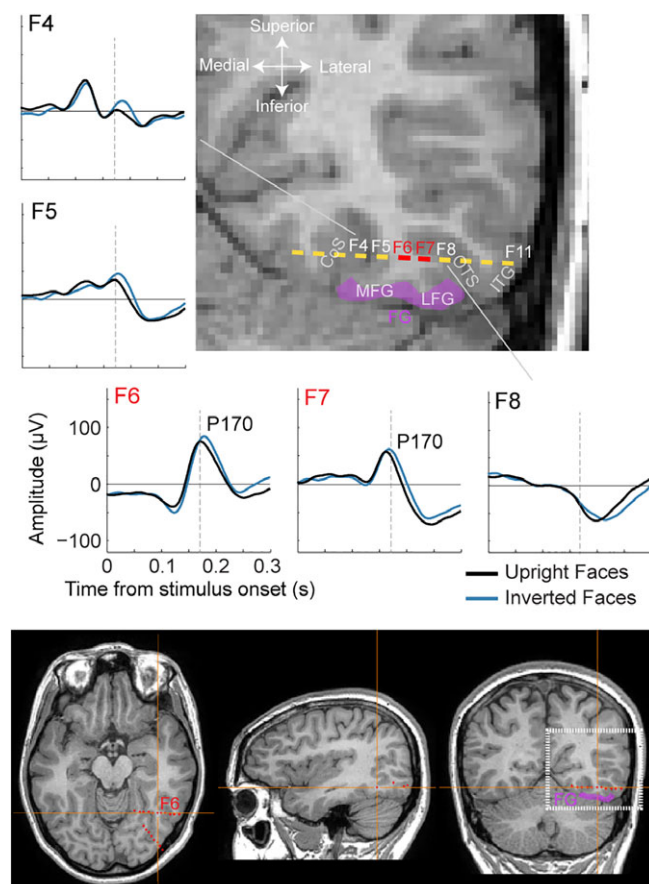
FIGURE 7 A P170 measured above the lateral fusiform gyrus (FG). (a) Averaged ERP responses to upright and inverted faces in five intracerebral contacts of the F electrode (F4–F8), passing from the collateral sulcus to the OTS above the FG. The anatomical location of the contacts from the F electrodes is shown on a coronal slide. Contacts F6 and F7 (highlighted in red), which are at the border of the OTS 8 mm above the inferior surface of the lateral FG show a prominent P170 component. The FG is highlighted in purple color. (b) Location of the F6 intracerebral contact relative to the patient's brain and head (see Figure 1 for additional anatomical details) [Color figure can be viewed at wileyonlinelibrary.com]

dense and even coverage of bilateral OT scalp regions. This scalp coverage over the OT region has been demonstrated to orthogonally project to the IOG (Koessler et al., 2009).

This data set is rare for several reasons. First, simultaneous IOG and LFG electrode implantation are rare, given that occipital lobe epilepsies are a very rare form of drug-refractory focal epilepsies. Second, simultaneous intracerebral and scalp recordings with sufficient scalp coverage are even scarcer because of fear of secondary infection. Third, compared to SEEG used here, ECoG—which has been the more widely used surgical method to record human intracranial electrophysiology—is suboptimal for simultaneous scalp–intracranial recordings. Indeed, the extensive craniotomies involved for placing ECoG grids/strips generally prevent from using high-density recordings and create large discontinuities in the skull which are known to distort the EEG signal on the scalp (e.g., Flemming et al., 2005). Such difficulties are minimized with SEEG (e.g., Dubarry et al., 2014).

Although the observations reported here are described in a single case patient with refractory epilepsy, we argue that they can be

generalized to other (healthy) adult brains. Indeed, this patient appears to have a typically (i.e., similar to healthy normal adults) functioning face-selective brain network, as demonstrated by the following observations: this patient has: (a) a typical cortical face network as defined in fMRI (Jonas et al., 2012, 2014), (b) a large and typical scalp N170 with a right hemispheric dominance, (c) a typical N170 FIE (Figure 2), and (d) fully preserved face recognition skills as revealed with neuropsychological tests (see Jonas et al., 2012). Finally, electrical stimulation of the OFA in the right IOG of this patient impaired her ability to recognize familiar famous faces (Jonas et al., 2012) or to discriminate individual unfamiliar faces (Jonas et al., 2014), in line with the observation that acquired prosopagnosia is most frequently associated with brain lesions to this region (Bouvier & Engel, 2006) and can result from focal lesions to this region (Rossion et al., 2003). Yet, additional simultaneous EEG–SEEG measurements in other patients in similar experimental setups and a wide range of cortical geometry and spatial sampling of cortical activity are needed to ensure full generalizability of our observations.

4.2 | The right IOG is a major cortical source of the scalp N170

Overall, this data set provides direct evidence against the claim that only the P1, not the N170 evoked by faces is generated in the right IOG, and that the N170 would rather originate from the middle FG (Duchaine & Yovel, 2015; Pitcher et al., 2011; Sadeh et al., 2010; Yovel, 2016). As noted in Section 1, this serial/hierarchical view for the spatiotemporal organization of the cortical face network is based on the following observations: (a) correlational measures performed between (face-selective) responses on the OT scalp in EEG and in the IOG and FG in fMRI (Horovitz et al., 2004; Sadeh et al., 2010), (b) the early latency of TMS effects applied to the IOG on face processing (Pitcher et al., 2008, 2007), as well as (c) source localization of the N170/M170 mostly in the FG (Deffke et al., 2007; Halgren et al., 2000; Henson et al., 2009; Herrmann et al., 2005; Hoshiyama et al., 2003; Itier et al., 2006; Mnatsakanian & Tarkka, 2004; Pizzagalli et al., 2002; Rossion, Joyce, et al., 2003; Shibata et al., 2002; Watanabe et al., 2003).

Why do our observations fail to align with these previous findings? First, Sadeh et al. (2010) report that the magnitude of fMRI face selectivity in the IOG correlates with OT region EEG face selectivity only during the P1 time window (being significant in a single time-bin at 112 ms after stimulus onset), while fMRI face selectivity in the FG correlates with EEG responses only during the N170 time window (160–180 ms after stimulus onset). One key aspect that may have contributed to differences in findings between Sadeh et al. (2010) and the present study is that Sadeh et al. correlated EEG to fMRI using a metric of face selectivity computed for each subject while we directly correlated the absolute amplitude/latency of the N170. The correlation approach in the present study (i.e., using variability in trials measured simultaneously across channels) prevents from using such a metric (e.g., an index of face inversion) as responses to upright and inverted faces were measured in separate trials. Interestingly, a more recent attempt to correlate simultaneously recorded EEG and fMRI during face processing using raw amplitude rather than face selectivity also failed to find a strong relationship between the amplitude of the

BOLD signal in the FFA and the amplitude of the scalp N170 (Nguyen & Cunnington, 2014). In addition, Sadeh et al. (2010) prevented from having deviant face-selectivity index (i.e., outside [−1 1] range) due to the N170 being sometimes of opposite sign in response to face and nonface stimuli, by subtracting a constant value to the whole sample of N170 amplitude. This procedure can potentially have a strong impact on the face-selectivity index (especially for small N170 amplitudes), and resulting correlation values with small number of data points are unwarranted. Another important difference is that in Sadeh et al. (2010), correlations were performed using across-subjects variability (N = 10), while our study relies on within-subject across-trial variability of the N170 latency and amplitude, a more direct way of assessing the correspondence across these measurements. Finally, Sadeh et al. (2010) investigate the relationship between IOG and scalp-level responses using two very different signals (EEG vs. fMRI) with very different temporal properties, while the present study measured electrophysiological signals of the same nature on the scalp and inside the brain.

A second line of evidence for the serial/hierarchical view of face processing comes from observations that TMS double pulses directed to the OFA impairs performance in different face processing tasks only when these pulses are sent at 60 and 100 ms after face onset, but not when pulses are sent at 20 and 60 ms or 100 and 140 ms (Pitcher et al., 2008, 2007). The authors interpreted these observations as evidence that the OFA processes face information in the time window of the P1 component (typically 80–120 ms), thus before the N170 component. However, the pattern of performance modulation as a function of time in these studies strongly suggest that: (a) the first pulse at 60 ms is insufficient to significantly disrupt face processing (because it is not disrupted in the 20–60 ms pulse condition), and (b) it is the second TMS pulse (sent at 100 ms), adding up to the first pulse, that effectively generates the behavioral impairment. This indicates that the critical time window for disrupting face processes in the OFA is 100–140 ms, when the N170 rises, rather than strictly in the P1 time window. Such an interpretation would in fact be compatible with the current finding that a major source of the scalp N170 lies in the lateral IOG. In addition, this interpretation would also be compatible with the current finding that the N170 in the IOG and P170 above the LFG have very similar latencies (i.e., 160–170 ms, Figure 4), in line with the finding of simultaneous (or even earlier) face-selective response onsets in the FFA compared to the OFA with time-resolved fMRI (Gentile et al., 2017; Jiang et al., 2011, 2015).

Finally, the majority of electromagnetic source imaging studies of scalp EEG or MEG activity report main sources of the N170/M170 around the posterior to anterior FG (Deffke et al., 2007; Henson et al., 2009; Herrmann et al., 2005; Itier et al., 2006; Mnatsakanian & Tarkka, 2004; Rossion, Joyce, et al., 2003; Shibata et al., 2002; Watanabe et al., 2003), although some report main or additional sources in the IOG (Henson et al., 2009; Itier et al., 2006; Rossion, Joyce, et al., 2003) or the posterior STS (Itier & Taylor, 2004; Watanabe et al., 2003). However, the ill-posed nature of the inverse problem and the diversity in source imaging algorithms (see Grech et al., 2008 for a review) make it difficult to draw firm conclusions about the relative involvement of the IOG and FG regions (which are spatially close to each other and are likely to have correlated responses) in

generating the scalp N170. Interestingly, numerous intracranial electrophysiological studies have reported face-selective negativities around 170–200 ms (N170 or N200, Allison et al., 1994, 1999; Davidesco et al., 2014; Miller, Schalk, Hermes, Ojemann, & Rao, 2016; Privman et al., 2007; Puce et al., 1999; Rangarajan et al., 2014; Rosburg et al., 2010) from posterior to anterior sections of the FG. However, none of these studies has reported scalp EEG data in order to establish a contribution of these intracranial FG responses to the scalp N170 (but see Rosburg et al., 2010 for simultaneous recording of FG and vertex scalp location). Our current findings of a major contribution of the lateral IOG in generating the scalp N170 are therefore not incompatible with the recording of large N170/N200 responses in the FG. Our findings are, however, directly in line with the few reports of N170 responses in the lateral IOG (Rosburg et al., 2010; Sato et al., 2014), as well as with the observation of a robust increase in the N170 amplitude and latency for inverted relative to upright faces in this region (Rosburg et al., 2010).

We acknowledge that our claim of the IOG as a major source for the scalp N170 seems incompatible with the finding of a preserved face-selective scalp N170 despite completely missing right IOG face-selective region in the brain-lesioned prosopagnosic patient PS (Prieto et al., 2011). However, it is fair to say that, contrary to the current case (Figure 2), PS's N170 showed both an abnormal scalp topography (which is found also for other face-selective responses and is likely to be related to the lesion in PS's skull over the right OT region; see Liu-Shuang, Torfs, & Rossion, 2016; Sorger, Goebel, Schiltz, & Rossion, 2007) and a reduced face-selectivity, suggesting that the IOG is still critical in generating a "normal" N170, in line with the current findings and with other sources of evidence in brain damaged prosopagnosic patients (Dalrymple et al., 2011). Moreover, since the N170 amplitude varies substantially across individuals, one cannot exclude that patient PS's N170 was much larger before her brain damage.

4.3 | Potential contribution of the LFG to the OT scalp N170

Given that we report data from a single patient implanted only with three intracerebral electrode arrays, our finding of the lateral IOG as a major source of the scalp N170 does not rule out the contribution of other cortical sources, including potential sources in or around the LFG. Indeed, it is clear that robust face-selective responses are generated in the LFG, as indicated both with fMRI (e.g., Gao et al., 2018; Kanwisher et al., 1997; Rossion et al., 2012; Weiner & Grill-Spector, 2010) and intracranial electrophysiology (Allison et al., 1994, 1999; Davidesco et al., 2014; Jacques et al., 2016; Jonas et al., 2016; Miller, Hermes, Pestilli, Wig, & Ojemann, 2017; Privman et al., 2007; Rangarajan et al., 2014). Moreover, these electrophysiological face-selective responses often occur between 100 and 200 ms following stimulus onset, with clear peaks at about 160–170 ms. Here, we would like to discuss some of the conditions that determine the potential contribution of the LFG to the scalp OT N170. In light of these, we argue that, in the current patient, the contribution of the LFG is likely minimal.

First, if the LFG strongly contributed to the scalp OT N170, we should have observed a correlation between the P170 amplitude (negative correlation) or latency (positive correlation) measured at F6 or

F7 and the N170 measured on the scalp OT regions. However, we did not observe such correlations. It is fair to say here that the spatial sampling of the LFG in this patient was far from complete. However, although it is possible that our sparse intracerebral sampling of the LFG may have missed the bulk of the face-selective responses in this region, we still measured a clear P170 component with an effect of face inversion at F6 and F7. Moreover, even though, the location of the LFG contacts may not have been optimal and the distance of these contacts from scalp OT electrodes is larger than with contacts in the IOG—likely weakening putative correlations—, we still may have expected a weak correlation between LFG and scalp OT channels.

Second, one should consider the local geometry of the cortical folding in this area, as this determines the orientation of the electrical fields generated in this region relative to the scalp surface. The LFG has the majority of its external cortical surface pointing toward the inferior part of the head (or toward more medial aspects of the head due to the cerebellum under it). In line with Bentin et al.'s (1996) original proposal, we argue that the electrical field (dipole) generating the N200–N170 component on the ventral surface of the LFG is oriented roughly vertically (i.e., perpendicular to the inferior cortical surface), with the negative pole pointing toward the bottom of the head (or the center of the neck when the LFG surface is slightly oblique), which is geometrically incompatible with a strong contribution of the LFG to the OT scalp N170. This hypothesis is supported by current and previous intracranial EEG studies: while SEEG studies using similar intracerebral electrodes as electrode F here, passing over or slightly above the internal/superior surface of the FG, consistently report a positive component (P170, Barbeau et al., 2008; Halgren et al., 1994), ECoG studies with electrodes placed over the external/inferior surface of the FG consistently report a negative component (N170 or N200, e.g., Allison et al., 1994, 1999; Miller et al., 2016; Rangarajan et al., 2014; Rosburg et al., 2010). In the current patient, the finding of a P170 sensitive to face inversion in contacts above the LFG provides original supports for this hypothesis by refuting the possibility that the P170 in LFG contacts is generated by a mediolateral dipole pointing to the lateral OT scalp surface. Indeed, the ERP response in contacts located just medially (in CoS) and laterally (in OTS and ITG) to FG contacts do no exhibit a component with a similar morphology or latency (Figures 3a and 7), suggesting that the P170 in LFG contacts is not generated by a dipole oriented along the mediolateral axis.

Although the argument about cortical geometry of the LFG makes it unlikely for this region to be a major contributor to the scalp OT N170, it does not completely rule out a potential contribution of the medial banks of the mid-fusiform sulcus (MFS) or the OTS around the FG region to the scalp N170. In most individuals, including patient KV of the present study, the FG is subdivided into a medial and lateral section by a small sulcus located along the posterior–anterior axis: the MFS (Weiner et al., 2014). While the (small) cortical surface of the medial bank of the MFS does point toward the lateral scalp OT region, its contribution to the face-sensitive N170 is unlikely. Indeed, the medial and lateral banks of the MFS are part of two distinct cytoarchitectonic structures (FG3 and FG4, respectively, Lorenz et al., 2017), with face-selective responses in the LFG being largely confined to the lateral bank of the MFS. In addition, potential neural sources located in the OTS, laterally to the FG, and generating a horizontal or oblique

electrical field, may very well contribute to the N170 measured on OT scalp electrodes (Bentin et al., 1996). Indeed, fMRI face-selective activation in the LFG frequently spreads to the medial bank of the OTS (e.g., Gao et al., 2018; Weiner & Grill-Spector, 2010; Zhen et al., 2015). However, the large difference in peak latency between the scalp N170 (around 160 ms) and the negativity measured in the OTS (F8-F9: 180–200 ms), as well as the absence of a scalp-like N170 component in contacts lateral to the OTS (F10-F11) in the current patient do not bring support for such a contribution.

In the present study, we provide clear evidence for a major contribution of the IOG to the scalp OT N170. However, establishing the nature of the contribution of the FG region to this ERP component needs further exploration. As indicated earlier, we report the data from a single patient with a single intracerebral multicontact electrode passing over the FG, which may have missed other neural sources in the FG. To complement our findings, one approach would be to take advantage of the methodological tools developed here, where future studies would combine high-density scalp recordings and intracerebral recordings at different OT locations in larger groups of patients. A complementary approach would be to rely on forward source modeling, combining detailed modeling of the individual cortical geometry and head, with simulating the activation of distinct face-selective regions in the OT cortex (see Ales, Yates, & Norcia, 2010 for primary visual cortex simulations).

As a final note, while the FG may only minimally contribute to the OT scalp N170, this region may contribute to the face-sensitive VPP measured over the vertex, located above the FG, at the same time window as the N170, the two components sharing functional properties (Jeffreys, 1989, 1996; Joyce & Rossion, 2005). Unfortunately, here, we found no significant correlation between the P170 measured in contacts F6 and F7 and the signal at central scalp electrodes (e.g., Cz, Fz, Figures 5 and 6). However, these scalp electrodes are relatively far from the FG and signal quality at these channels was rather poor. Further studies investigating scalp to intracerebral relationship are needed to determine whether the FG distinctively contributes to the VPP, or if this component which shares functional properties with the N170 despite reduced sensitivity, emerges essentially at this location due to the use of reference electrodes near the OT regions (earlobes or mastoids, see Joyce & Rossion, 2005).

ORCID

Corentin Jacques https://orcid.org/0000-0001-8917-4346
Bruno Rossion https://orcid.org/0000-0002-1845-3935

REFERENCES

Ales, J. M., Yates, J. L., & Norcia, A. M. (2010). V1 is not uniquely identified by polarity reversals of responses to upper and lower visual field

stimuli. *NeuroImage*, *52*, 1401–1409. https://doi.org/10.1016/j.neuroimage.2010.05.016

Allison, T., Ginter, H., McCarthy, G., Nobre, A. C., Puce, A., Luby, M., & Spencer, D. D. (1994). Face recognition in human extrastriate cortex. *Journal of Neurophysiology*, *71*, 821–825.

Allison, T., Puce, A., Spencer, D. D., McCarthy, G., & Belger, A. (1999). Electrophysiological studies of human face perception. I: Potential generated in occipitotemporal cortex by face and non-face stimuli. *Cerebral Cortex*, *9*, 415–430.

Barbeau, E. J., Taylor, M. J., Regis, J., Marquis, P., Chauvel, P., & Liégeois-Chauvel, C. (2008). Spatio temporal dynamics of face recognition. *Cerebral Cortex*, *18*, 997–1009. https://doi.org/10.1093/cercor/bhm140

Bentin, S., McCarthy, G., Perez, E., Puce, A., & Allison, T. (1996). Electrophysiological studies of face perception in humans. *Journal of Cognitive Neuroscience*, *8*, 551–565.

Botzel, K., & Grusser, O. J. (1989). Electric brain potentials-evoked by pictures of faces and non-faces – A search for face-specific EEG-potentials. *Experimental Brain Research*, *77*, 349–360.

Botzel, K., Schulze, S., & Stodieck, S. R. G. (1995). Scalp topography and analysis of intracranial sources of face-evoked potentials. *Experimental Brain Research*, *104*, 135–143.

Bouvier, S. E., & Engel, S. A. (2006). Behavioral deficits and cortical damage loci in cerebral achromatopsia. *Cerebral Cortex*, *16*, 183–191.

Calder, A. J., & Young, A. W. (2005). Understanding the recognition of facial identity and facial expression. *Nature Reviews Neuroscience*, *6*, 641–651.

Dalrymple, K. A., Oruç, I., Duchaine, B., Pancaroglu, R., Fox, C. J., Iaria, G., … Barton, J. J. (2011). The anatomic basis of the right face-selective N170 in acquired prosopagnosia: A combined ERP/fMRI study. *Neuropsychologia*, *49*, 2553–2563. https://doi.org/10.1016/j.neuropsychologia.2011.05.003

Davidesco, I., Zion-Golumbic, E., Bickel, S., Harel, M., Groppe, D. M., Keller, C. J., … Malach, R. (2014). Exemplar selectivity reflects perceptual similarities in the human fusiform cortex. *Cerebral Cortex*, *24*, 1879–1893. https://doi.org/10.1093/cercor/bht038

Deffke, I., Sander, T., Heidenreich, J., Sommer, W., Curio, G., Trahms, L., & Lueschow, A. (2007). MEG/EEG sources of the 170-ms response to faces are co-localized in the fusiform gyrus. *NeuroImage*, *35*, 1495–1501.

Dubarry, A., Badier, J., Fonseca, A. T., Gavaret, M., Carron, R., Bartolomei, F., … Bénar, C. G. (2014). Simultaneous recording of MEG, EEG and intracerebral EEG during visual stimulation: From feasibility to single-trial analysis. *NeuroImage*, *99*, 548–558. https://doi.org/10.1016/j.neuroimage.2014.05.055

Duchaine, B., & Yovel, G. (2015). A revised neural framework for face processing. *Annual Review of Vision Science*, *1*, 393–416. https://doi.org/10.1146/annurev-vision-082114-035518

Eimer, M. (2000). Effects of face inversion on the structural encoding and recognition of faces – Evidence from event-related brain potentials. *Cognitive Brain Research*, *10*, 145–158.

Feuerriegel, D., Churches, O., Hofmann, J., & Keage, H. A. D. (2015). The N170 and face perception in psychiatric and neurological disorders: A systematic review. *Clinical Neurophysiology*, *126*, 1141–1158. https://doi.org/10.1016/j.clinph.2014.09.015

Flemming, L., Wang, Y., Caprihan, A., Eiselt, M., Haueisen, J., & Okada, Y. (2005). Evaluation of the distortion of EEG signals caused by a hole in the skull mimicking the fontanel in the skull of human neonates. *Clinical Neurophysiology*, *116*, 1141–1152. https://doi.org/10.1016/j.clinph.2005.01.007

Ganis, G., Smith, D., & Schendan, H. E. (2012). The N170, not the P1, indexes the earliest time for categorical perception of faces, regardless of interstimulus variance. *NeuroImage*, *62*, 1563–1574. https://doi.org/10.1016/j.neuroimage.2012.05.043

Gao, X., Gentile, F., & Rossion, B. (2018). Fast periodic stimulation (FPS): A highly effective approach in fMRI brain mapping. *Brain Structure & Function*, *223*, 2433–2454. https://doi.org/10.1007/s00429-018-1630-4

Gao, Z., Goldstein, A., Harpaz, Y., Hansel, M., Zion-Golumbic, E., & Bentin, S. (2013). A magnetoencephalographic study of face processing: M170, gamma-band oscillations and source localization. *Human Brain Mapping*, *34*, 1783–1795. https://doi.org/10.1002/hbm.22028

Gauthier, I., Tarr, M. J., Moylan, J., Skudlarski, P., Gore, J. C., & Anderson, A. W. (2000). The fusiform "face area" is part of a network that processes faces at the individual level. *Journal of Cognitive Neuroscience*, *12*, 495–504. https://doi.org/10.1162/089892900562165

Gentile, F., Ales, J., & Rossion, B. (2017). Being BOLD: The neural dynamics of face perception. *Human Brain Mapping*, *38*, 120–139. https://doi.org/10.1002/hbm.23348

George, N., Evans, J., Fiori, N., Davidoff, J., & Renault, B. (1996). Brain events related to normal and moderately scrambled faces. *Cognitive Brain Research*, *4*, 65–76.

Grech, R., Cassar, T., Muscat, J., Camilleri, K. P., Fabri, S. G., Zervakis, M., … Vanrumste, B. (2008). Review on solving the inverse problem in EEG source analysis. *Journal of NeuroEngineering and Rehabilitation*, *33*, 1–33. https://doi.org/10.1186/1743-0003-5-25

Grill-Spector, K., Weiner, K. S., Kay, K., & Gomez, J. (2017). The functional neuroanatomy of human face perception. *Annual Review of Vision Science*, *3*, 167–196. https://doi.org/10.1146/annurev-vision-102016-061214

Halgren, E., Baudena, P., Heit, G., Clarke, J. M., Marinkovic, K., Chauvel, P., & Clarke, M. (1994). Spatio-temporal stages in face and word processing. 2. Depth-recorded potentials in the human frontal and Rolandic cortices. *Journal of Physiology, Paris*, *88*, 51–80.

Halgren, E., Raij, T., Marinkovic, K., Jousmaki, V., & Hari, R. (2000). Cognitive response profile of the human fusiform face area as determined by MEG. *Cerebral Cortex*, *10*, 69–81.

Haxby, J. V., Hoffman, E. A., & Gobbini, M. I. (2000). The distributed human neural system for face perception. *Trends in Cognitive Sciences*, *4*, 223–233.

Henson, R. N., Mouchlianitis, E., & Friston, K. J. (2009). MEG and EEG data fusion: Simultaneous localisation of face-evoked responses. *NeuroImage*, *47*, 581–589. https://doi.org/10.1016/j.neuroimage.2009.04.063

Herrmann, M. J., Ehlis, A. C., Muehlberger, A., & Fallgatter, A. J. (2005). Source localization of early stages of face processing. *Brain Topography*, *18*, 77–85.

Horovitz, S. G., Rossion, B., Skudlarski, P., & Gore, J. C. (2004). Parametric design and correlational analyses help integrating fMRI and electrophysiological data during face processing. *NeuroImage*, *22*, 1587–1595. https://doi.org/10.1016/j.neuroimage.2004.04.018

Hoshiyama, M., Kakigi, R., Watanabe, S., & Miki, K. (2003). Brain responses for the subconscious recognition of faces. *Neuroscience Research*, *46*, 435–442. https://doi.org/10.1016/S0168-0102(03)00121-4

Itier, R. J., Herdman, A. T., George, N., Cheyne, D., & Taylor, M. J. (2006). Inversion and contrast-reversal effects on face processing assessed by MEG. *Brain Research*, *1115*, 108–120.

Itier, R. J., & Taylor, M. J. (2004). N170 or N1? Spatiotemporal differences between object and face processing using ERPs. *Cerebral Cortex*, *14*, 132–142. https://doi.org/10.1093/cercor/bhg111

Jacques, C., & Rossion, B. (2007). Early electrophysiological responses to multiple face orientations correlate with individual discrimination performance in humans. *NeuroImage*, *36*, 863–876.

Jacques, C., Schiltz, C., & Goffaux, V. (2014). Face perception is tuned to horizontal orientation in the N170 time window. *Journal of Vision*, *14*(2), 5, 1-18. https://doi.org/10.1167/14.2.5

Jacques, C., Witthoft, N., Weiner, K. S., Foster, B. L., Rangarajan, V., Hermes, D., … Grill-Spector, K. (2016). Corresponding ECoG and fMRI category-selective signals in human ventral temporal cortex. *Neuropsychologia*, *83*, 14–28. https://doi.org/10.1016/j.neuropsychologia.2015.07.024

Jeffreys, D. (1989). A face-responsive potential recorded from the human scalp. *Experimental Brain Research*, *78*, 193–202. https://doi.org/10.1007/BF00230699

Jeffreys, D. (1996). Evoked potential studies of face and object processing. *Visual Cognition*, *3*, 1–38.

Jiang, F., Badler, J. B., Righi, G., & Rossion, B. (2015). Category search speeds up face-selective fMRI responses in a non-hierarchical cortical face network. *Cortex*, *66*, 69–80.

Jiang, F., Dricot, L., Weber, J., Righi, G., Tarr, M. J., Goebel, R., & Rossion, B. (2011). Face categorization in visual scenes may start in a higher order area of the right fusiform gyrus: Evidence from dynamic

visual stimulation in neuroimaging. *Journal of Neurophysiology*, 106, 2720–2736. https://doi.org/10.1152/jn.00672.2010

Jonas, J., Descoins, M., Koessler, L., Colnat-Coulbois, S., Sauvée, M., Guye, M., ... Maillard, L. (2012). Focal electrical intracerebral stimulation of a face-sensitive area causes transient prosopagnosia. *Neuroscience*, 222, 281–288. https://doi.org/10.1016/j.neuroscience.2012.07.021

Jonas, J., Jacques, C., Liu-shuang, J., Brissart, H., Colnat-Coulbois, S., & Maillard, L. (2016). A face-selective ventral occipito-temporal map of the human brain with intracerebral potentials. *Proceedings of the National Academy of Sciences of the United States of America*, 113, E4088–E4097. https://doi.org/10.1073/pnas.1522033113

Jonas, J., Rossion, B., Krieg, J., Koessler, L., Colnat-Coulbois, S., Vespignani, H., ... Maillard, L. (2014). Intracerebral electrical stimulation of a face-selective area in the right inferior occipital cortex impairs individual face discrimination. *NeuroImage*, 99, 487–497. https://doi.org/10.1016/j.neuroimage.2014.06.017

Joyce, C., & Rossion, B. (2005). The face-sensitive N170 and VPP components manifest the same brain processes: The effect of reference electrode site. *Clinical Neurophysiology*, 116, 2613–2631.

Kanwisher, N., McDermott, J., & Chun, M. M. (1997). The fusiform face area: A module in human extrastriate cortex specialized for face perception. *The Journal of Neuroscience: The Official Journal of the Society for Neuroscience*, 17, 4302–4311. https://doi.org/10.1098/Rstb.2006.1934

Koessler, L., Cecchin, T., Colnat-Coulbois, S., Vignal, J.-P., Jonas, J., Vespignani, H., ... Maillard, L. G. (2015). Catching the invisible: Mesial temporal source contribution to simultaneous EEG and SEEG recordings. *Brain Topography*, 28, 5–20. https://doi.org/10.1007/s10548-014-0417-z

Koessler, L., Maillard, L., Benhadid, A., Vignal, J. P., Felblinger, J., Vespignani, H., & Braun, M. (2009). Automated cortical projection of EEG sensors: Anatomical correlation via the international 10 – 10 system. *NeuroImage*, 46, 64–72. https://doi.org/10.1016/j.neuroimage.2009.02.006

Liu, J., Higuchi, M., Marantz, A., & Kanwisher, N. (2000). The selectivity of the occipitotemporal M170 for faces. *Neuroreport*, 11, 337–341.

Liu-Shuang, J., Torfs, K., & Rossion, B. (2016). An objective electrophysiological marker of face individualisation impairment in acquired prosopagnosia with fast periodic visual stimulation. *Neuropsychologia*, 83, 100–113. https://doi.org/10.1016/j.neuropsychologia.2015.08.023

Lorenz, S., Weiner, K. S., Caspers, J., Mohlberg, H., Schleicher, A., Bludau, S., ... Amunts, K. (2017). Two new cytoarchitectonic areas on the human mid-fusiform gyrus. *Cerebral Cortex*, 27, 373–385. https://doi.org/10.1093/cercor/bhv225

McCarthy, G., Puce, A., Belger, A., & Allison, T. (1999). Electrophysiological studies of human face perception. II: Response properties of face-specific potentials generated in occipitotemporal cortex. *Cerebral Cortex*, 9, 431–444.

Miller, J., Patterson, T. U. I., & Ulrich, R. (1998). Jackknife-based method for measuring LRP onset latency differences. *Psychophysiology*, 35, 99–115.

Miller, K. J., Hermes, D., Pestilli, F., Wig, G. S., & Ojemann, J. G. (2017). Face percept formation in human ventral temporal cortex. *Journal of Neurophysiology*, 118, 2614–2627. https://doi.org/10.1152/jn.00113.2017

Miller, K. J., Schalk, G., Hermes, D., Ojemann, J. G., & Rao, R. P. N. (2016). Spontaneous decoding of the timing and content of human object perception from cortical surface recordings reveals complementary information in the event-related potential and broadband spectral change. *PLoS Computational Biology*, 12, e1004660. https://doi.org/10.1371/journal.pcbi.100, https://doi.org/10.1371/journal.pcbi.1004660

Mnatsakanian, E. V., & Tarkka, I. M. (2004). Familiar-face recognition and comparison: Source analysis of scalp-recorded event-related potentials. *Clinical Neurophysiology*, 115, 880–886. https://doi.org/10.1016/j.clinph.2003.11.027

Mouraux, A., & Iannetti, G. D. (2008). Across-trial averaging of event-related EEG responses and beyond. *Magnetic Resonance Imaging*, 26, 1041–1054.

Nguyen, V. T., & Cunnington, R. (2014). The superior temporal sulcus and the N170 during face processing: Single trial analysis of concurrent EEG – fMRI. *NeuroImage*, 86, 492–502. https://doi.org/10.1016/j.neuroimage.2013.10.047

Nichols, T. E., & Holmes, A. P. (2001). Nonparametric permutation tests for functional neuroimaging experiments: A primer with examples. *Human Brain Mapping*, 15, 1–25. https://doi.org/10.1002/hbm.1058

Pitcher, D., Garrido, L., Walsh, V., & Duchaine, B. C. (2008). Transcranial magnetic stimulation disrupts the perception and embodiment of facial expressions. *The Journal of Neuroscience*, 28, 8929–8933. https://doi.org/10.1523/JNEUROSCI.1450-08.2008

Pitcher, D., Walsh, V., & Duchaine, B. (2011). The role of the occipital face area in the cortical face perception network. *Experimental Brain Research*, 209, 481–493. https://doi.org/10.1007/s00221-011-2579-1

Pitcher, D., Walsh, V., Yovel, G., & Duchaine, B. (2007). TMS evidence for the involvement of the right occipital face area in early face processing. *Current Biology*, 17, 1568–1573. https://doi.org/10.1016/j.cub.2007.07.063

Pizzagalli, D. a., Lehmann, D., Hendrick, A. M., Regard, M., Pascual-Marqui, R. D., & Davidson, R. J. (2002). Affective judgments of faces modulate early activity (∼160 ms) within the fusiform gyri. *NeuroImage*, 16, 663–677. https://doi.org/10.1006/nimg.2002.1126

Prieto, E. A., Caharel, S., Henson, R., & Rossion, B. (2011). Early (n170/m170) face-sensitivity despite right lateral occipital brain damage in acquired prosopagnosia. *Frontiers in Human Neuroscience*, 5, 138. https://doi.org/10.3389/fnhum.2011.00138

Privman, E., Nir, Y., Kramer, U., Kipervasser, S., Andelman, F., Neufeld, M. Y., ... Malach, R. (2007). Enhanced category tuning revealed by intracranial electroencephalograms in high-order human visual areas. *The Journal of Neuroscience*, 27, 6234–6342. https://doi.org/10.1523/JNEUROSCI.4627-06.2007

Puce, A., Allison, T., Bentin, S., Gore, J. C., & McCarthy, G. (1998). Temporal cortex activation in humans viewing eye and mouth movements. *The Journal of Neuroscience*, 18, 2188–2199.

Puce, A., Allison, T., Gore, J. C., & McCarthy, G. (1995). Face-sensitive regions in human extrastriate cortex studied by functional MRI. *Journal of Neurophysiology*, 74, 1192–1199.

Puce, A., Allison, T., & McCarthy, G. (1999). Electrophysiological studies of human face perception. III: Effects of top-down processing on face-specific potentials. *Cerebral Cortex*, 9, 445–458.

Rangarajan, V., Hermes, D., Foster, B. L., Weiner, K. S., Jacques, C., Grill-Spector, K., & Parvizi, J. (2014). Electrical stimulation of the left and right human fusiform gyrus causes different effects in conscious face perception. *The Journal of Neuroscience*, 34, 12828–12836. https://doi.org/10.1523/JNEUROSCI.0527-14.2014

Rosburg, T., Ludowig, E., Dümpelmann, M., Alba-Ferrara, L., Urbach, H., & Elger, C. E. (2010). The effect of face inversion on intracranial and scalp recordings of event-related potentials. *Psychophysiology*, 47, 147–157. https://doi.org/10.1111/j.1469-8986.2009.00881.x

Rossion, B. (2014). Understanding face perception by means of human electrophysiology. *Trends in Cognitive Sciences*, 18, 310–318. https://doi.org/10.1016/j.tics.2014.02.013

Rossion, B., Caldara, R., Seghier, M., Schuller, A. M., Lazeyras, F., & Mayer, E. (2003). A network of occipito-temporal face-sensitive areas besides the right middle fusiform gyrus is necessary for normal face processing. *Brain*, 126, 2381–2395. https://doi.org/10.1093/brain/awg241

Rossion, B., Delvenne, J. F., Debatisse, D., Goffaux, V., Bruyer, R., Crommelinck, M., & Guérit, J. M. (1999). Spatio-temporal localization of the face inversion effect: An event-related potentials study. *Biological Psychology*, 50, 173–189.

Rossion, B., Gauthier, I., Tarr, M. J., Despland, P., Bruyer, R., Linotte, S., & Crommelinck, M. (2000). The N170 occipito-temporal component is delayed and enhanced to inverted faces but not to inverted objects: An electrophysiological account of face-specific processes in the human brain. *Neuroreport*, 11, 69–74.

Rossion, B., Hanseeuw, B., & Dricot, L. (2012). Defining face perception areas in the human brain: A large-scale factorial fMRI face localizer analysis. *Brain and Cognition*, 79, 138–157. https://doi.org/10.1016/j.bandc.2012.01.001

Rossion, B., & Jacques, C. (2008). Does physical interstimulus variance account for early electrophysiological face sensitive responses in the

human brain? Ten lessons on the N170. *NeuroImage*, *39*, 1959–1979. https://doi.org/10.1016/j.neuroimage.2007.10.011

Rossion, B., & Jacques, C. (2011). The N170: Understanding the time-course of face perception in the human brain. In E. S. Kappenman & S. J. Luck (Eds.), *The Oxford handbook of ERP components* (pp. 115–142). New York, NY: Oxford University Press.

Rossion, B., Joyce, C. A., Cottrell, G. W., & Tarr, M. J. (2003). Early laterali-zation and orientation tuning for face, word, and object processing in the visual cortex. *NeuroImage*, *20*, 1609–1624. https://doi.org/10.1016/j.neuroimage.2003.07.010

Rousselet, G., Husk, J. S., Bennett, P. J., & Sekuler, A. B. (2008). Time course and robustness of ERP object and face differences. *Journal of Vision*, *8*(12), 3, 1–18. https://doi.org/10.1167/8.12.3

Rousselet, G. A., Mace, M. J. M., & Fabre-Thorpe, M. (2004). Animal and human faces in natural scenes: How specific to human faces is the N170 ERP component? *Journal of Vision*, *4*, 13–21.

Sadeh, B., Podlipsky, I., Zhdanov, A., & Yovel, G. (2010). Event-related potential and functional MRI measures of face-selectivity are highly correlated: A simultaneous ERP-fMRI investigation. *Human Brain Mapping*, *31*, 1490–1501. https://doi.org/10.1002/hbm.20952

Sadeh, B., & Yovel, G. (2010). Why is the N170 enhanced for inverted faces? An ERP competition experiment. *NeuroImage*, *53*, 782–789. https://doi.org/10.1016/j.neuroimage.2010.06.029

Salado, A. L., Koessler, L., De Mijolla, G., Schmitt, E., Vignal, J.-P., Civit, T., ... Colnat-Coulbois, S. (2018). sEEG is a safe procedure for a compre-hensive anatomic exploration of the insula: A retrospective study of 108 procedures representing 254 transopercular insular electrodes. *Operative Neurosurgery*, *14*, 1–8. https://doi.org/10.1093/ons/opx106

Sato, W., Kochiyama, T., Uono, S., Matsuda, K., Usui, K., Inoue, Y., & Toichi, M. (2014). Rapid, high-frequency, and theta-coupled gamma oscillations in the inferior occipital gyrus during face processing. *Cortex*, *60*, 1–17. https://doi.org/10.1016/j.cortex.2014.02.024

Seeck, M., Koessler, L., Bast, T., Leijten, F., Michel, C., Baumgartner, C., ... Beniczky, S. (2017). The standardized EEG electrode array of the IFCN. *Clinical Neurophysiolog*y, *128*, 2070–2077. https://doi.org/10.1016/j.clinph.2017.06.254

Sergent, J., Ohta, S., & Macdonald, B. (1992). Functional neuroanatomy of face and object processing – A positron emission tomography study. *Brain*, *115*, 15–36.

Shibata, T., Nishijo, H., Tamura, R., Miyamoto, K., Eifuku, S., Endo, S., & Ono, T. (2002). Generators of visual evoked potentials for faces and eyes in the human brain as determined by dipole localization. *Brain Topography*, *15*, 51–63.

Sorger, B., Goebel, R., Schiltz, C., & Rossion, B. (2007). Understanding the functional neuroanatomy of acquired prosopagnosia. *NeuroImage*, *35*, 836–852.

Srebro, R. (1985). Localization of visually evoked cortical activity in humans. *Journal of Physiology*, *360*, 233–246.

Swithenby, S. J., Bailey, A. J., Brautigam, S., Josephs, O. E., Jousmaki, V., & Tesche, C. D. (1998). Neural processing of human faces: A magnetoen-cephalographic study. *Experimental Brain Research*, *118*, 501–510.

Talairach, J., & Bancaud, J. (1973). Stereotaxic approach to epilepsy. Meth-odology of anatomo-functional stereotaxic investigations. *Progress in Neurological Surgery*, *5*, 297–354. https://doi.org/https://doi.org/10.1159/000394343

Tanskanen, T., Nasanen, R., Montez, T., Paallysaho, J., & Hari, R. (2005). Face recognition and cortical responses show similar sensitivity to noise spatial frequency. *Cerebral Cortex*, *15*, 526–534.

Watanabe, S., Kakigi, R., & Puce, A. (2003). The spatiotemporal dynamics of the face inversion effect: A magneto- and electro-encephalographic study. *Neuroscience*, *116*, 879–895.

Weiner, K. S., Golarai, G., Caspers, J., Chuapoco, M. R., Mohlberg, H., Zilles, K., ... Grill-Spector, K. (2014). The mid-fusiform sulcus: A land-mark identifying both cytoarchitectonic and functional divisions of human ventral temporal cortex. *NeuroImage*, *84*, 453–465. https://doi.org/10.1016/j.neuroimage.2013.08.068

Weiner, K. S., & Grill-Spector, K. (2010). Sparsely-distributed organization of face and limb activations in human ventral temporal cortex. *Neuro-Image*, *52*, 1559–1573. https://doi.org/10.1016/j.neuroimage.2010.04.262

Yang, Y., Qiu, Y., & Schouten, A. C. (2015). Dynamic functional brain connectivity for face perception. *Frontiers in Human Neuroscience*, *9*, 662. https://doi.org/10.3389/fnhum.2015.00662

Yovel, G. (2016). Neural and cognitive face-selective markers: An integra-tive review. *Neuropsychologia*, *83*, 5–13. https://doi.org/10.1016/j.neuropsychologia.2015.09.026

Zhen, Z., Yang, Z., Huang, L., Kong, X., Wang, X., Dang, X., ... Liu, J. (2015). Quantifying interindividual variability and asymmetry of face-selective regions: A probabilistic functional atlas. *NeuroImage*, *113*, 13–25. https://doi.org/https://doi.org/10.1016/j.neuroimage.2015.03.010